WSRC-TR-2004-00164
Revision 0

Keywords: Tank Farm
Characterization
Salt Dissolution
Low Curie Salt

Retention: Permanent

Tank 10H Saltcake Core Sample Analysis

C. J. Martino
R. L. Nichols
D. J. McCabe
M. R. Millings

Publication date: April 19, 2004

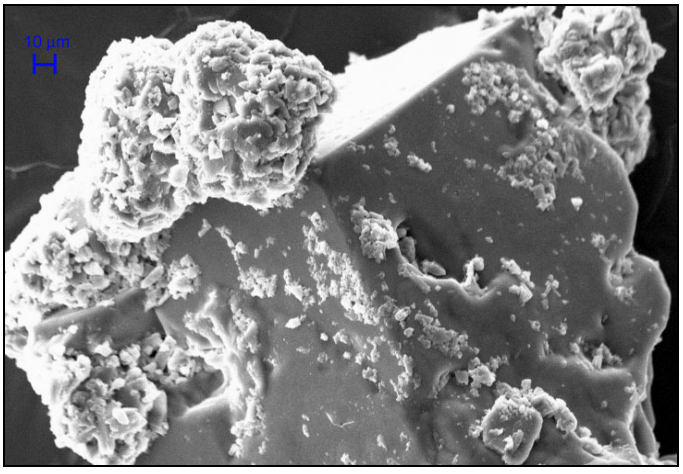

Westinghouse
Savannah River Company
Aiken, SC 29808

SRS
savannah river site
™

Summary

This report provides details of the characterization of the Tank 10H saltcake samples (HTF-609, 610, and 611) pulled in October 2003. These samples represent the top three 1-foot segments of the saltcake. The following are the major conclusions of this analysis:

- The three Tank 10H saltcake samples were filled to nearly their capacity, with an average bulk density of 2.06 g/cm^3.

- The undrained bulk saltcake from the top of the middle sample (HTF-610) had a water content of 12.8 wt %, a ^{137}Cs activity of 0.94 Ci per gallon of saltcake, an actinide content of 1.3E+6 pCi/g, and a ^{235}U enrichment of 6.6%. The unique characteristic of HTF-610 was the relatively large amount of sulfate (24 wt %) and carbonate (12 wt %), and the relatively small amount of nitrate (24 wt %).

- The undrained bulk saltcake from the bottom of the bottom sample (HTF-611) had a water content of 4.4 wt %, a ^{137}Cs activity of 0.63 Ci per gallon of saltcake, an actinide content of 1.1E+5 pCi/g, and a ^{235}U enrichment of 23%. HTF-611 had a more typical level of nitrate (64 wt %).

- Interstitial liquid drained from the top sample (HTF-609) had a density of 1.43 g/cm^3, a soluble solids content of 47.0 wt %, a ^{137}Cs activity of 3.3 Ci per gallon of interstitial liquid, and an actinide content of 2.6E+4 pCi/mL. Similar results were obtained for interstitial liquid drained from HTF-610.

- A flow-through dissolution test was performed on the drained saltcake sample from the bottom of HTF-609. The ^{137}Cs concentration was highest in the effluent from the earliest stages of dissolution and decreased during subsequent stages of the dissolution test, with the bulk dissolved salt effluent having a ^{137}Cs of 0.10 Ci/gal at 4.3 M [$Na^{+]}$ (corresponding to 0.14 Ci/gal at 6 M [Na^+]).

- The average hydraulic conductivity of the top portion of sample HTF-609 was 4.2 * 10^{-4} cm/sec, which is similar to that for a fine to medium grained sand.

- An estimated 91% of the residual ^{137}Cs in the drained salt sample HTF-609 was displaced by 2.9 pore volumes of simulated interstitial liquid during the falling head permeability test.

- Material from each of the three Tank 10H saltcake samples was analyzed by Scanning Electron Microscopy and X-ray Diffraction. Grain size and coherence are among the most notable physical differences within this 36 inch saltcake core, likely influencing the amount of macroporosity and microporosity. The material from the top of HTF-609, the top of the core sample, has large, loose, distinct grains. In contrast, sample HTF-611, from the bottom of the core, is more consolidated with numerous small precipitates covering and perhaps cementing larger grains together.

- Residual insoluble solids from the drained and dissolved Tank 10H sample HTF-609 contained sodium aluminosilicates, calcium aluminosilicates, mercury, iron, chrome, uranium, and a variety of other components.

This page was intentionally left blank

Table of Contents

List of Figures

List of Tables

List of Abbreviations

AA	Atomic Absorption spectroscopy
ADDS	Adjusted Drained Dissolved Salt
adj	adjusted
ADS	Analytical Development Section
DDS	Drained Dissolved Salt
DI	de-ionized
EDS	X-ray Emission Dispersive Spectroscopy
FL	Free Liquid supernatant to a saltcake sample upon receipt
HLW	High Level Waste
IC	Ion Chromatography
ICP-ES	Inductively-Coupled Plasma – Emission Spectroscopy
ICP-MS	Inductively-Coupled Plasma – Mass Spectroscopy
I.D.	inner diameter
IL	Interstitial Liquid drained from a saltcake sample
ILD	Interstitial Liquid Displacement
LCS	Low-Curie Salt
LWD	Liquid Waste Disposition
mes	measured
nd	not determined
nm	not measured
O.D.	outer diameter
PIL	Partitioned into the Interstitial Liquid
RBOF	Receiving Basin for Offsite Fuels
SEM	Scanning Electron Microscopy
SIL	Simulated (non-radioactive) Interstitial Liquid
SPF	Saltstone Processing Facility
SRS	Savannah River Site
SRTC	Savannah River Technology Center
TIC	Total Inorganic Carbon
TOC	Total Organic Carbon
UDS	Un-drained Dissolved Salt
WCS	Waste Characterization System
XRD	X-Ray Diffraction spectroscopy

Introduction

In support of Low-Curie Salt (LCS) process validation at the Savannah River Site (SRS), Liquid Waste Disposition (LWD) has undertaken a program of tank characterization, including salt sampling.[1,2] As part of this initiative, they sampled the surface and subsurface of Tank 10H saltcake using a series of three ~12-inch long sample tubes. These tubes each contain 1-foot long segments of the saltcake from one location, representing the top 3 feet of saltcake. The primary objective of the characterization is to gather information that will be useful to the selection and processing of the next waste tanks. Most important is the determination of the ^{137}Cs concentration and liquid retention properties of Tank 10H saltcake to confirm acceptability for processing. Additional chemical analyses are performed to provide information on salt elemental, ionic, and radiological composition to aid in assessment of the suitability of processing drained and dissolved material and in refining the information in the waste characterization system (WCS).

Background

Tank 10H is a Type I tank in the H tank farm and was previously a drop tank for the 1H-evaporator system. Tank 10H originally contained a greater quantity of saltcake, but a density-driven dissolution demonstration was performed in 1979 by the addition of Receiving Basin for Offsite Fuels (RBOF) waste from Tank 23H.[3,4] At the time of sampling, Tank 10H contained approximately 71 inches of salt and no supernate, and the saltcake temperature was 30 °C.

Samples

On October 23, 2003, three salt core samples were collected from Riser 3 of Tank 10H. These samples were contained in 0.99 in. inner diameter (I.D.), 1.13 in. outer diameter (O.D.), 13.7 in. long carbon steel tubes with capped ends. The top 2 inches of these sample tubes contained a thicker portion of threaded tubing. This 2-inch portion contained no sample material because it was attached to the mast during sampling.

The samples were delivered to the Savannah River Technology center (SRTC), placed into the Shielded Cells (Block B, Cell 8), and weighed on October 24th. Table 1 contains a description of the three Tank 10H samples documented in this report. Note that the sample volume is approximate because the depth to the salt in the top of the samples was determined by inserting a pipette and assuming that the surface was flat. Likewise, Figure 1 displays the approximate contents of the Tank 10H samples and indicates the regions within the samples that were used for the initial bulk saltcake and moisture content characterization.

Figure 2 shows, from left to right, the bottom of HTF-609, the top and bottom of HTF-610, and the bottom of HTF-611. Figure 3 shows the salt removed for characterization from the bottom of HTF-611 and the top of HTF-610.

Salt at the bottom of HTF-609 was slightly off-white in color. This salt was easily scooped from the sample tube end, it glistened slightly, and it lightly adhered to surfaces such as the spatula or tube. The salt was not runny or soupy. Observation of salt from the top of HTF-609, performed after vacuum draining of the sample, revealed a white, dry, granular material that was easily poured from the top of the tube. This material appeared translucent with individual grains, similar to typical sand or sugar.

Salt from the top of HTF-610 was dark gray and slightly moist, though not runny. It was the darkest area of the sample that we observed. It was easily removed from the sample tube and, despite the difference in appearance, it behaved similarly to salt from the top of HTF-609. Salt from the bottom of

HTF-610 was white, in sharp contrast to the salt from the top of HTF-610. After sample draining, the sample was severed near its middle, revealing salt that was nearer to the appearance of that from the bottom of HTF-610.

Salt from the bottom of HTF-611 was a white and hard-packed powder that was not easily scooped form the sample tube. When removed, it appeared as an opaque, dry, fluffy powder that did not adhere to surfaces. No observation was made of the salt from the top of HTF-611 due to the extra threaded length of the tube.

Table 1: Tank 10H Sample Description

Relative Location	Tank Farm Name	Tube Name	Salt Mass (g)	Volume (cm^3)	Density (g/cm^3)
top	HTF-609	HTF-E-03-117	290.11	143.0	2.03
middle	HTF-610	HTF-E-03-118	308.89	142.3	2.17
bottom	HTF-611	HTF-E-03-119	288.09	145.4	1.98
total			887.09	430.6	2.06

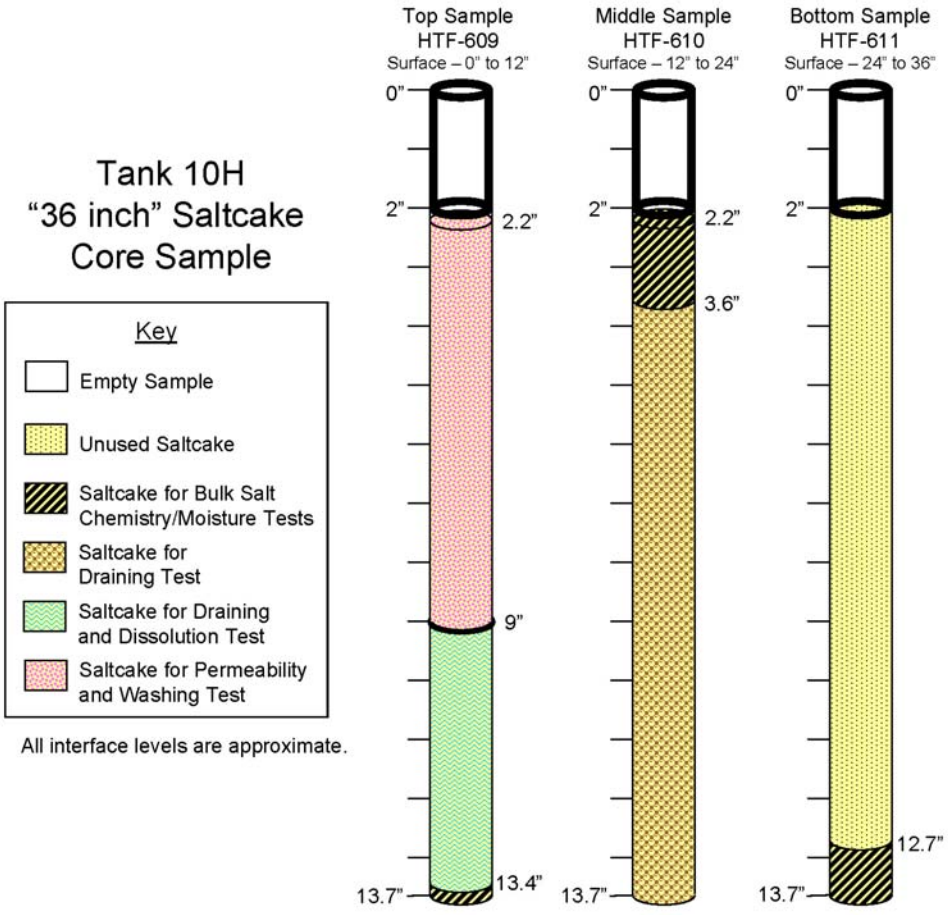

Figure 1: Material contained in Tank 10H core samples

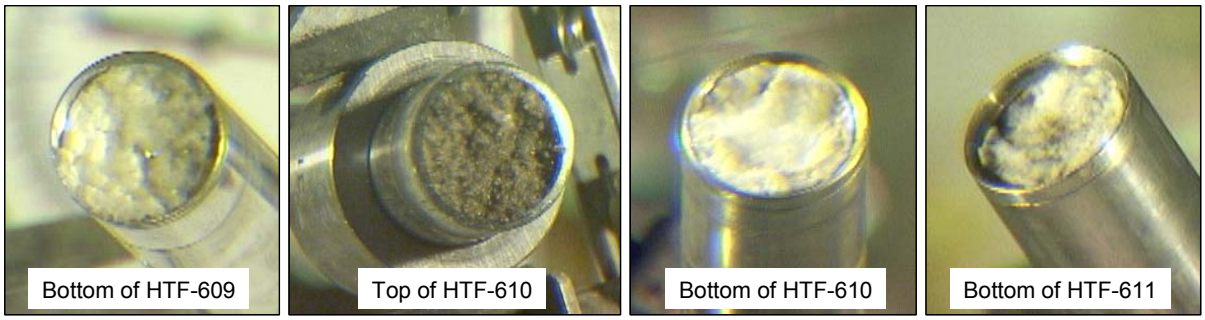

Figure 2: Tank 10H saltcake from the bottom of HTF-609, the top of HTF-610, the bottom of HTF-610, and the bottom of HTF-611.

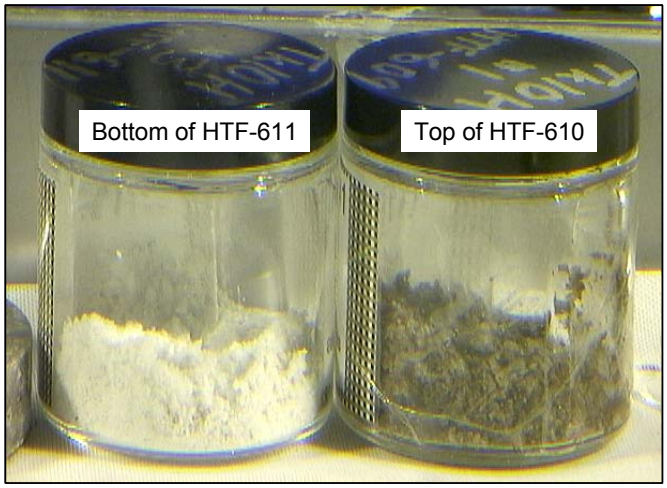

Figure 3: Salt collected from the bottom of HTF-611 and the top of HTF-610.

Experimental

Chemical and Radiological Analysis

The sample was weighed, uncapped, and visually inspected upon receipt in the shielded cells. Material from the bottom of HTF-609 was removed and dried for water content. The top of sample tube HTF-610 was cut off and the material from the top of HTF-610 was sampled. Material from the bottom of HTF-611 was sampled. The material from the bottom of HTF-610 and HTF-611 were used for both the undrained bulk saltcake chemical and radiological characterization and water content measurements. Samples HTF-609 and HTF-610 were drained under vacuum to remove a portion of the interstitial liquid from the solid salt. Drained interstitial liquid from HTF-609 was also used for chemical and radiological characterization and water content measurements.

Undrained bulk salt characterization was performed on salt removed from the top of HTF-610 and the bottom of HTF-611. The characterization included water content measurement and chemical/radiochemical analyses. Undrained bulk salt subsamples were prepared for analysis either by aqua regia (acid) dissolution or by DI water dissolution. The dissolutions were performed by dissolving approximately 2 grams of the material into 100 mL of liquid. For the DI water dissolutions, aliquots were taken from the liquid portion after agitation and settling, although no significant residual solids were visible. The aqua regia dissolutions were submitted to radiological chemistry for ^{137}Cs

(gamma scan), Pu isotopics, ^{241}Am, and ^{90}Sr, inductively coupled plasma – emission spectroscopy (ICP-ES) for elemental analysis, inductively coupled plasma – mass spectroscopy (ICP-MS) for certain actinide and fission product quantification, and atomic absorption (AA) spectroscopy for the measurement of As, Se, Hg, and K. The water dilutions/dissolutions were submitted for ion chromatography (IC) for anion characterization, wet chemistry/titration for total base, free hydroxide, and CO_3^{2-} analysis, and total inorganic and organic carbon (TIC/TOC) analysis. An additional portion of the water-dissolved sample was submitted for ^{14}C analysis. Similar analyses were performed on the filtered interstitial liquid that was drained from HTF-609.

To obtain a total concentration, several analytes require assumptions to be made or calculations from multiple analytical methods. The ^{99}Tc is reported as a maximum value based on the entire mass 99 data from ICP-MS, and thus ignores any contribution of ^{99}Ru. If there were any natural abundance ruthenium present, the amount would be in proportion to the mass 101 values. Since it is not possible to determine the amount of natural and fission product ruthenium, it is not feasible to calculate the contribution of ^{99}Ru to the mass 99 value. In any event, the contribution is likely small as the mass 101 value rarely exceeds 5% of the mass 99 value. The ^{135}Cs is reported as a maximum value based on the entire mass 135 data, and thus ignores any contribution of ^{135}Ba. This provides a good measurement for the filtered liquid samples because of the limited Ba solubility. Total Cs is calculated as the sum of ^{133}Cs from ICP-MS and ^{137}Cs from radiochemistry. The calculation of total Cs does not contain the ^{135}Cs contribution, which is always relatively small (<10 wt% of total Cs). The total strontium in the saltcake sample was estimated based on the ICP-MS measurement of mass 88, assuming a natural abundance of ^{86}Sr and ^{87}Sr, and combining it with the mass of ^{90}Sr from radiochemistry counting. This causes a small overestimation of the total strontium as the ^{86}Sr and ^{87}Sr would actually be less abundant because some of the ^{88}Sr is present as a fission product. Total Co is reported as mass 59, and thus may be biased high in the presence of organic or inorganic components that fragment at mass 59. An alternative free hydroxide estimate is provided as a calculated value by taking the total base and subtracting the contribution of aluminate and carbonate ions. Total inorganic carbon is reported as mass of CO_3^{2-} and total organic carbon is reported as mass of carbon.

Draining in Vacuum Extraction Cell

Interstitial liquid (IL) was extracted from samples HTF-609 and HTF-610 using 8” Hg vacuum for 4 and 10 days respectively. Eight inches of Hg corresponds to 78 inches of interstitial liquid in the tank and is consistent with the vacuum used to drain other samples allowing a qualitative comparison of drainage characteristics for salt samples from different tanks. A 100 mesh stainless steel screen was placed in the bottom shipping cap to retain salt particles in the sample tube during vacuum extraction. Figure 4 shows the apparatus used to extract the IL. Drainage was terminated when the weight of the volumetric flask with IL was constant. The density and mass fraction of water were determined for the extracted IL.

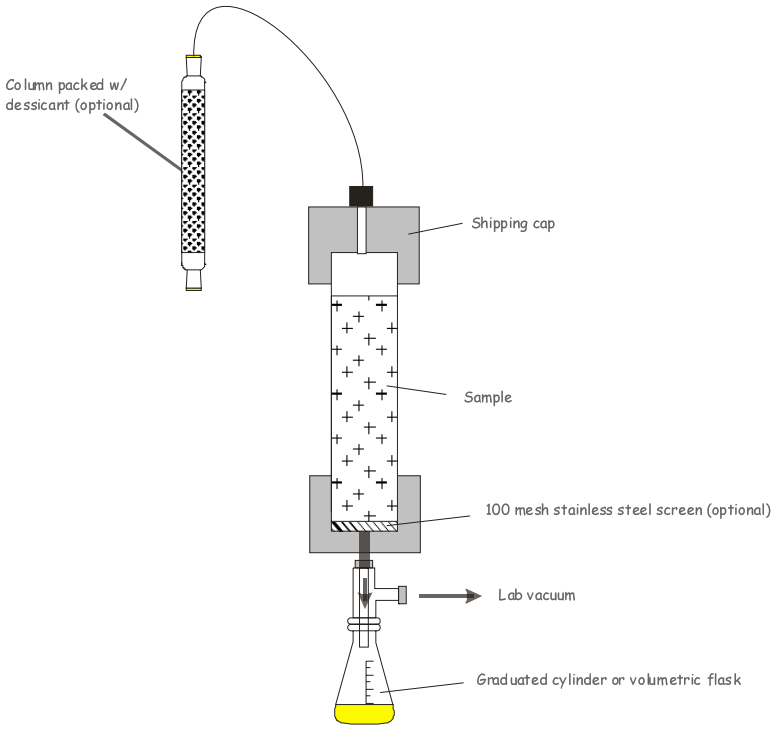

Figure 4: Apparatus used to extract interstitial liquid from saltcake samples.

Physical Properties Analysis

Density, Moisture, and Percent Interstitial Liquid

The saltcake bulk density of the as-received material was calculated using the weight of sample obtained and an estimate of the filled volume of the tube. Density of the interstitial liquid was measured as the weight of material required to fill 2 mL Class A volumetric flasks. The water content of the saltcake and the drained interstitial liquid were estimated gravimetrically: small portions (~1g) of saltcake were dried at 115 °C (±5 °C) to drive off water until a constant weight had been achieved.

Samples of drained salt were collected from the top and bottom of each sample to determine the final water content. Interstitial liquid content was then calculated using the density of IL and mass fraction of water in IL.

Porosity and Saturation

The porosity and saturation of saltcake samples were estimated using the following equations.

$$\phi = \frac{V_{voids}}{V_{total}} = \frac{V_{total} - V_{solid}}{V_{total}} \quad (1)$$

$$V_{solid} = \frac{W_{solid}}{\rho_{solid}} = \frac{W_{total} - W_{liquid}}{\rho_{solid}} \quad (2)$$

$$W_{liquid} = \left(\frac{W_{total} * \theta_{water}}{\chi_{wil}} \right) \quad (3)$$

$$S = \frac{V_{liquid}}{V_{voids}} = \frac{\left(\frac{W_{liquid}}{\rho_{liquid}} \right)}{\left(V_{total} * \phi \right)} \quad (4)$$

S = saturation (fraction)
ϕ = porosity (fraction)
ρ_{soild} =density of solids
ρ_{liquid} =density of liquid
χ_{wlL}= mass fraction of water in interstitial liquid
θ_w = gravimetric water content
V_{total} = total volume of sample
V_{solid} = volume of solids in sample
V_{voids} = volume of sample that does not correspond to solids
V_{liquid} = volume of liquid in sample
W_{total} = total weight of sample
W_{solid} = weight of solids in sample
W_{liquid} = weight of interstitial liquid in sample

Permeability

A falling-head permeability test was conducted on the top half sample HTF-609 to measure its permeability. The falling-head permeameter was constructed in the High-Level Shielded Cells in SRTC and incorporated the as-received sample tube in the permeameter. The permeability test method was similar to that used on saltcake samples from Tank 41H.[5] The hydraulic conductivity is a function of the fluid (density and viscosity) and the porous matrix, while the permeability is a function of only the porous media and is independent of the fluid properties. The falling-head permeameter allows for the measurement of the hydraulic conductivity of the sample for the specific interstitial liquid. Simulated interstitial liquid (SIL) was used to saturate the saltcake in an effort to replace the interstitial liquid that had been drained while minimizing the interaction and potential dissolution of the porous saltcake matrix. The SIL used to saturate the sample was a 10.8 M [Na^+] solution with a [OH^-]/[NO_3^-] of 4.5 and density of 1.4 g/ml, Table 2. The sample was saturated with 28 ml of SIL from the bottom up over a period of 15 days.

Table 2: Chemical composition of simulated interstitial liquid used to saturated saltcake samples for falling head permeability test.

Component	Concentration
NaOH	6.8 M
$NaNO_3$	1.5 M
$NaNO_2$	2.5 M

After the sample was saturated, the falling head apparatus was assembled (see Figure 5). A burette was used as the SIL reservoir and a standpipe with overflow was connected to the top of the sample to maintain a constant pressure on the discharge side of the sample. The scale on the burette was measured prior to placement in the shielded cells so the volume readings could be converted to length for use in permeability calculations. The burette was refilled 8 times during the testing, allowing for a total of 10 permeability calculations. During the test, a total of 56.2 mL (3 pore volumes) of fluid was passed through the sample.

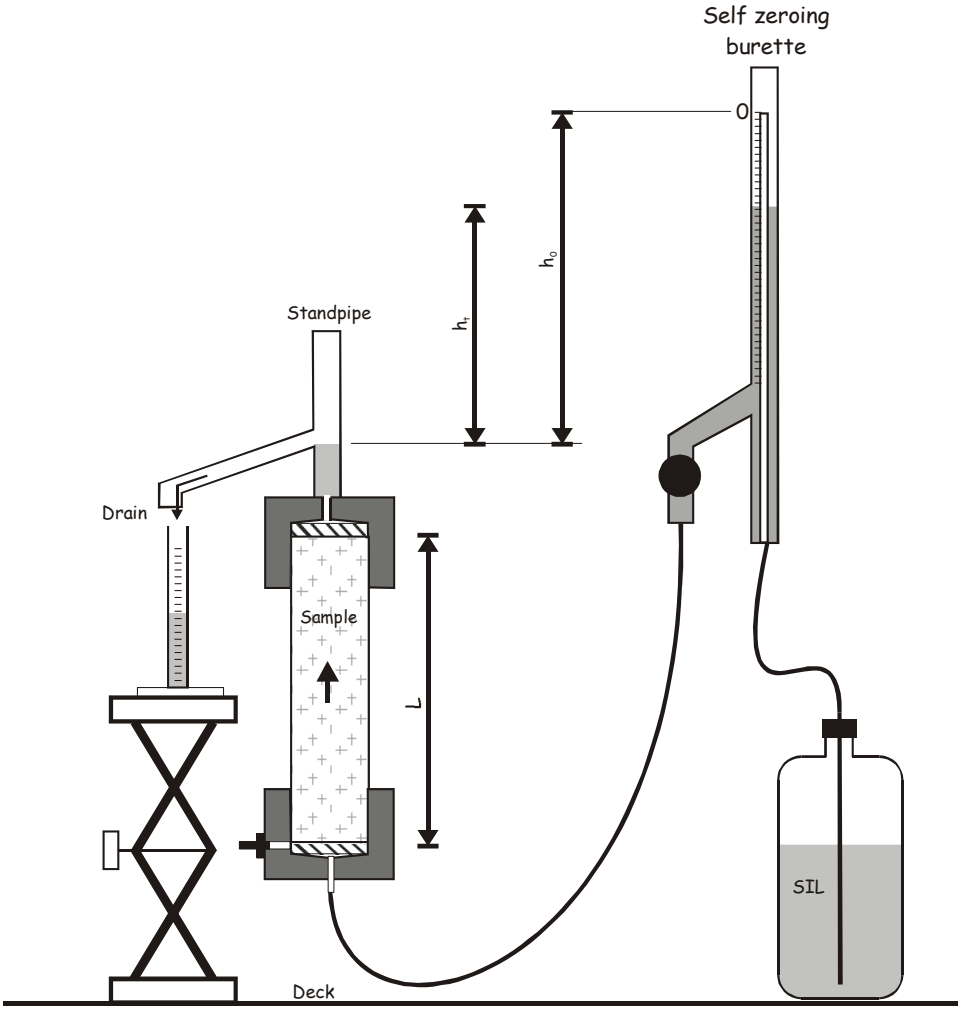

Figure 5: Falling Head Apparatus Used To Test Saltcake Samples.

Six effluent samples collected during the continuous sampling of effluent from the falling head test were analyzed using gamma spectroscopy for Cs-137 and ICP-ES for elemental analysis. Each of the samples was diluted ~20:1 wt/wt with 2M HNO_3 prior to leaving the shielded cells for analysis by the Analytical Development Section (ADS) of SRTC.

Dissolution of Drained Saltcake

Figure 6 contains a generalized illustration of the apparatus used during dissolution testing of the bottom portion of the drained sample HTF-609. The apparatus utilized a 4.7 inch long portion of the salt core sample contained in the original ~1 inch I.D., 1/16 inch wall thickness sampling tube. The dissolution apparatus was essentially the same as the vacuum-extraction apparatus, with the exception of the media bag for water introduction. Salt was removed from the bottom of HTF-609 for water content measurement prior to dissolution testing. The dissolution of the bottom portion of HTF-609 was performed in an orientation that was inverted from the in-tank orientation of the sample so that the larger void would be at the top of the apparatus, allowing better water-solid contact. No screen was used at the bottom of the sample during the dissolution protocol.

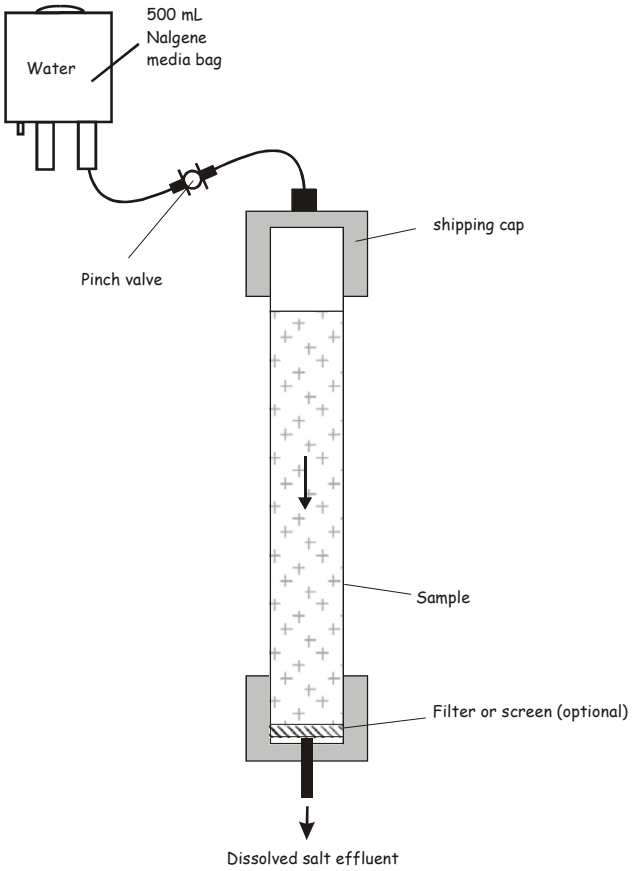

Figure 6: Rough schematic of dissolution test apparatus.

DI water was introduced to the top of the sample tube via a media bag and the dissolved salt effluent was collected from the bottom of the sample. The rate of water introduction could be roughly controlled by a pinch valve, but the rate of effluent elution can be limited by the saltcake physical properties. In most cases, gravity is the primary force driving the fluid through pores and channels in the dissolving saltcake. In some instances, however, liquid would not be evident at the bottom of the sample after a significant period of time. In those cases, vacuum was applied to the bottom of the sample in a manner similar to the process for draining interstitial liquid from samples.

The dissolved salt effluent was periodically sampled in 5 mL aliquots. The collection of these aliquots was timed to obtain an estimate of the effluent flow rate. These aliquots were weighed to obtain the effluent density. During periods of salt dissolution when an aliquot was not collected, the dissolved salt effluent was collected in a larger graduated bottle. For the remainder of this report, the small

aliquots are referred to as sub-samples of drained/dissolved saltcake and the larger bottles of effluent are referred to as the bulk drained/dissolved saltcake.

Analysis of the composite bulk drained/dissolved saltcake was performed after filtration of the material through a 0.45-micron filter. Analysis of sub-samples taken at various stages throughout the flow-through dissolution process was performed without filtration. Subsamples were prepared for chemical and radiochemical analyses at 20 to 50-times dilutions with 2 M nitric acid and DI water. The nitric acid dilutions were submitted for the same analyses as were the acid dissolutions of the core samples. The analyses included radiological chemistry, ICP-ES, ICP-MS, and AA. The water dilutions of the filtered samples were submitted for IC, wet chemistry titration, and TIC/TOC. The filter was analyzed by microscopy and spectroscopy techniques to identify solid phases and particle size. Two values are reported for ^{99}Tc by ICP-MS: a maximum based on the entire mass 99 data as ^{99}Tc, and a minimum number adjusting for the potential ^{99}Ru assuming that the mass 101 result is from natural ^{101}Ru.

Microscopy and Spectroscopy

Portions of the saltcake samples were investigated by scanning electron microscopy (SEM) with energy dispersive spectroscopy (EDS). Preparation for SEM involved drying and plating the material with carbon. Note that this is in contrast to previous samples that were coated with gold-palladium. Also in contrast to previous saltcake samples, the Tank 10H saltcake was investigated with the new contained SEM (Leo model 440). Separate portions of the saltcake samples were investigated by X-ray diffraction (XRD). The residual insoluble solids filtered from the bulk drained and dissolved HTF-609 sample was also investigated by XRD and SEM.

Results and Discussion

Tabulated results for the undrained saltcake are reported in the report body and in the appendix as the average and the standard deviation of the analysis of triplicate dissolutions. The interstitial liquid results are reported as the average of one to three analyses of a single dilution or dissolution, with the standard deviation only appearing in the appendix. Values reported as their detection limits are preceded by "<" and values that contain an average of detectable concentrations and detection limits are preceded by "</=". Blank values in the tables, "--", are either not determined or not applicable.

Physical Analysis

Table 3 contains the density and water content results for the saltcake removed from the bottom of HTF-609, the top of HTF-610, and the bottom of HTF-611. It also contains the standard deviation of repeated measurements. These results show moisture content variations within the sample. By comparison with samples from Tanks 29H and 38H, the Tank 10H samples are relatively dry. The Tank 10H samples are more similar in moisture content to the samples from Tanks 2F and 3F. The water content values measured from sample drying are denoted by (mes). Additional estimated water content values are provided, denoted by (adj). These additional values are the adjusted water contents based on partitioning 100% of the ^{137}Cs into the interstitial liquid and assuming the interstitial liquid has a constant composition throughout the samples.

The bulk density of the saltcake samples from Tank 10H varied from 1.98 to 2.17 g/cm^3 and is consistent with the range of previously reported values for saltcake samples from other waste tanks (see Table 4). The middle sample from Tank 10H, HTF-610, had the highest bulk density of the three Tank 10H samples and represents the highest bulk density reported using the thin walled sampling tube technique. The increased bulk density is likely due to the higher content of sulfate and carbonate salts in the sample when compared to the Tanks 2F, 3F, and 41H samples and the bottom Tank 10H sample, were all predominately sodium nitrate salts. A larger IL content may also

contribute to the increased bulk density. Porosities calculated for the Tank 10H samples were slightly higher than those previously reported for other salt samples from waste tanks. The salt particle density of HTF-609 and HTF-611 was estimated to be 2.3 g/cm^3 for these predominately sodium nitrate salts. The HTF-610 was taken to have the salt particle density of a mixture of sodium nitrate and burkeite, or 2.45 g/cm^3. If the adjusted water content values are used, the Tank 10H samples had a nearly constant porosity (26 to 28 vol %) and saturations that varied from 74 vol % for the bottom of HTF-611 to 94 and 97 vol % for the bottom of HTF-609 and the top of HTF-610, respectively.

Table 3: Density and Water/Liquid content of the Tank 10H samples (wt %)

Analyte	Unit	HTF-609						HTF-610				HTF-611	
		undrained saltcake		IL (filtered)		DDS (filtered)		undrained saltcake		IL (filtered)		undrained saltcake	
		average	stdev	average	stdev	average	stdev	average	stdev	average	stdev	average	stdev
Density	g/mL	2.03	--	1.435	0.002	1.23	--	2.17	--	1.438	--	1.98	--
Water (mes)	wt %	9.9%	0.2%	53.0%	0.2%	~74%	--	12.8%	0.5%	51.3%	0.2%	4.4%	0.04%
Liquid (mes)	wt %	18.8	--	100	--	100	--	25.1	--	100	--	8.3	--
Liquid (mes)	vol %	27	--	100	--	100	--	38	--	100	--	11	--
Water (adj)	wt %	9.9%	0.2%	53.0%	0.2%	~74%	--	8.6%	--	51.3%	0.2%	7.2%	--
Liquid (adj)	wt %	18.8	--	100	--	100	--	16.8	--	100	--	13.7	--
Liquid (adj)	vol %	27	--	100	--	100	--	25	--	100	--	19	--

(mes): water measured on undrained saltcake, (adj): water in undrained saltcake adjusted based on partitioning all Cs-137 into the IL

DDS water content was estimated from a mass balance summing individual anions and cations

water in wt% is θ_w for saltcake and χ_{wIL} for liquids.

Table 4: Physical properties of saltcake samples.

Tank	Sample ID	Sample Interval (ft)	Bulk Density (g/cm^3)	Water Content θ_w (wt %)	Porosity ϕ (vol %)	Saturation S (vol %)
10H	HTF-609	0-1	2.03	9.9 ± 0.2	28	94
	HTF-610	1-2	2.17	12.8 ± 0.5	38	> 100
	HTF-611	2-3	1.98	4.4 ± 0.04	21	55
	HTF-610	1-2	2.17	8.6 [b]	26	97
	HTF-611	2-3	1.98	7.2 [b]	26	74
29H	T29H-B6-1	0-1	2.13	21	nd	nd
2F	T2F-1-1	0-1	2.04	6.2 ± 0.6	23	77
3F	T3F-1-3	1-2	2.07	5.1 ± 2.6	19	76
41H	HTF-E-03-034	1-2	1.92[a]	3.2[a]	22	34

Note: θ_w reported as average $\pm$1 Std. Dev.
[a] average of results reported in Nichols et al., 2004.[5]
nd = not determined due to lack of data on salt particles
[b] θ_w was estimated assuming cesium is 100% partitioned into the IL

Chemical and Radiological Analysis

Undrained Saltcake

Table 11 through Table 16 contain the initial characterization information for the undrained bulk saltcake. Results are reported as the average of analyses of triplicate sample dissolutions.

The ^{137}Cs activities of salt from the top of HTF-610 and the bottom of HTF-611 were 1.14E+8 pCi/g (0.94 Ci/gal) and 8.36E+7 pCi/g (0.63 Ci/gal), respectively. The trend in ^{137}Cs activity roughly follows the trend in water content, with the wetter sample having more ^{137}Cs. This trend is evident for several other components, including K, PO_4^{3-}, and NO_2^-.

Although the two portions of saltcake were different in moisture content, appearance, and ^{137}Cs activity, perhaps the most significant difference between salt from the top of HTF-610 and the bottom of HTF-611 was the actinide content. Summing the ^{238}Pu, $^{239/240}Pu$, and ^{241}Am, the actinide content of the material from HTF-610 and HTF-611 were 1.3E+6 pCi/g and 1.1E+5 pCi/g, respectively. The ^{238}Pu activity, and thus the actinide content, is roughly an order-of-magnitude greater in HTF-610 than in HTF-611. The dark material from the top of HTF-610 was also rich in Mn, Fe, and Hg, which are more typically found in sludge than in saltcake.

The total uranium concentration was 0.0094 wt % for the dark portion of saltcake from the top of HTF-610 and only 0.0023 wt % in the light portion of saltcake from the bottom of HTF-611. The ^{235}U enrichment for HTF-610 was only 6.6%, however, which is much lower than the ^{235}U enrichment of HTF-611 (23%). The salt from both locations contained similar amounts of ^{235}U, but the salt from HTF-610 appeared to have additional ^{238}U present as well.

The other unique characteristic of the saltcake from the top of HTF-610 was the relatively large amount of sulfate (24 wt %) and carbonate (12 wt %), and a relatively small amount of nitrate (24 wt %) when compared with other HLW saltcake samples. Insoluble material remained in the water diluted HTF-610 sample used to obtain the IC anions, wet chemistry, and TIC/TOC results of Table 13. The saltcake from the bottom of HTF-611 contained a relatively large amount of oxalate (0.4 wt %), which should remain primarily insoluble until the later stages of Tank 10H salt dissolution.

The total strontium in the saltcake sample was calculated by adjusting the ICP-MS observation of ^{88}Sr assuming natural strontium isotopic ratios and adding the radiochemistry value for ^{90}Sr. The total strontium in the Tank 10H samples averaged 2.45E-4 wt %, of which ^{90}Sr had a 16.0 wt % isotopic contribution to the total strontium. Alternately, a total strontium analysis was available by ICP-ES as 5.70E-3 wt %, and the isotopic contribution of ^{90}Sr calculates to 0.7 wt %. The total strontium measured by these two independent means differ significantly. Further work is recommended to resolve this discrepancy.

Carbon-14 was spot checked on one sample from Tank 10H. The sample used was the material from HTF-610 that contained a large amount of carbonates and sulfates. The measured value of ^{14}C in HTF-610 was 2.2E+4 pCi/g. It is likely that the ^{14}C in other portions of the sample (such as HTF-611) would be lower due to the lower total carbon and carbonate content.

Interstitial Liquid

Table 17 through Table 20 contain the initial characterization information for the drained and filtered interstitial liquid (IL) from HTF-609. Approximately 17 grams of IL was drained from HTF-609 over a period of five days. The density of the interstitial liquid was 1.435 g/cm^3 with a standard deviation of 0.002 g/cm^3 determined from two measurements. The soluble solids content of the interstitial liquid was 47.0 wt % with a standard deviation of 0.2 wt % determined from three measurements. The

interstitial liquid was 9.5 M Na^+ and had a ^{137}Cs content of 8.79E+8 pCi/mL (3.3 Ci/gal). The ^{238}Pu content of 2.35E+4 pCi/mL in the interstitial liquid was much lower than that of the bulk saltcake from HTF-610 and HTF-611. The uranium content of the interstitial liquid was too low to determine the ^{235}U enrichment accurately.

Dissolution of Drained Saltcake

Samples HTF-609 and HTF-610 (the top and middle of the three Tank 10H samples, respectively) were drained under vacuum upon receipt into the Shielded Cells. At first, an attempt was made to dissolve the drained sample HTF-610. The larger void in the sample was at the top of the sample where the as-received analyses material had been removed, so the sample was dissolved in its in-tank orientation. Water was added to HTF-610 and vacuum was applied to force flow through the sample. After two shifts of vacuum-assisted dissolution, only a few mL of effluent emerged from the salt. The dissolution of HTF-610 was aborted.

After experiencing difficulty performing the Tank 10H dissolution test on HTF-610, it was decided to perform the testing on a portion of HTF-609. After as-received sampling, sample HTF-609 contained 290.11 g of undrained saltcake. HTF-609 was drained under 7 inches Hg vacuum for 3.7 days, removing 13.3 g of interstitial liquid. Sample HTF-609 was severed into two pieces so that the portion of salt contained in the bottom 4.75 inches of the sample tube would be utilized in the dissolution test. At the start of the dissolution test, approximately 104 g of drained saltcake remained in the bottom 4.75 inch portion of HTF-609.

There was a void at the bottom of the bottom portion of HTF-609 (salt had been removed for as-received analysis), so this sample was dissolved in an orientation inverted from its in-tank orientation in order to maximize liquid-solid contact. Water was added to the saltcake at nearly 3 mL/min and effluent started to flow from the apparatus within the first minute. Dissolution proceeded smoothly, but it was evident that there was little liquid holdup in the column. Figure 7 shows, from left to right, the first through sixth sub-sample and the bulk salt effluent collected during the dissolution of the Tank 10H drained sample HTF-609. These samples contained a small amount of solids. Prior to taking the photo, the samples had been agitated to re-suspend the solids. Figure 8 shows the solids settled at the bottom of the bulk salt effluent as a very small portion of the overall material.

Table 21 through Table 23, in the appendix, contain the Tank 10H sample HTF-609 dissolution information and chemical/radiochemical analyses of the unfiltered sub-samples and filtered bulk dissolved salt effluent. Density and sodium concentration declined over the course of the test. Figure 9 indicates that the nitrate, sulfate, and carbonate content in the dissolved salt sub-samples remained roughly constant throughout the test. As seen in Figure 9, the ^{137}Cs concentration decreased throughout the test and was faster than the decline in sodium concentration, as expected. The bulk dissolved salt effluent had a ^{137}Cs concentration of 0.10 Ci/gal at 4.3 M [Na^+], corresponding to 0.14 Ci/gal at 6 M [Na^+]. The total alpha content of the filtered bulk salt effluent was 5.4 nCi/mL. The alpha content of the filtered bulk salt effluent was more than 10-times less than the alpha content of the unfiltered sub-samples, indicating that some of the alpha activity can be removed by filtration in these experiments, although the dissolution time and temperature are not consistent with conditions in full-scale waste tank retrieval.

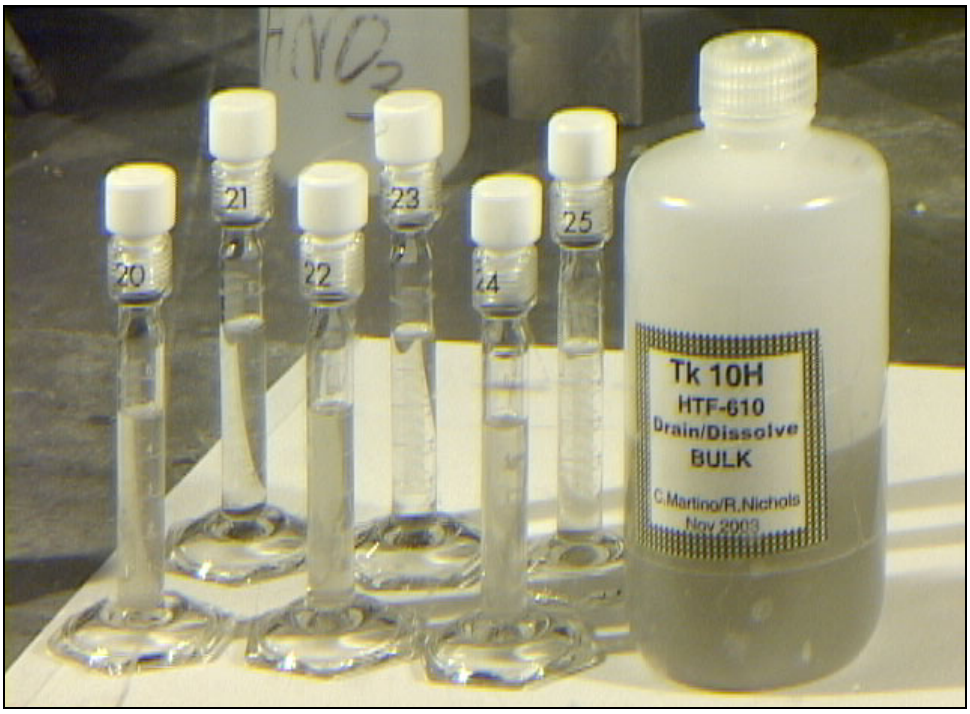

Figure 7: Tank 10H Dissolved Samples (material was from HTF-609, not HTF-610)

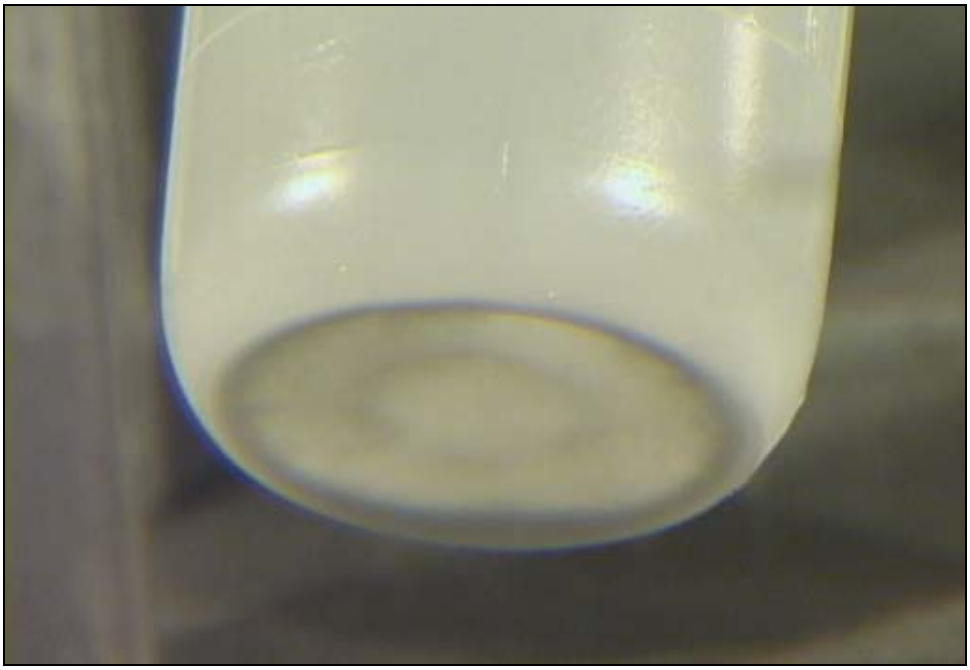

Figure 8: Settled Solids in Bulk Effluent from Tank 10H Dissolution

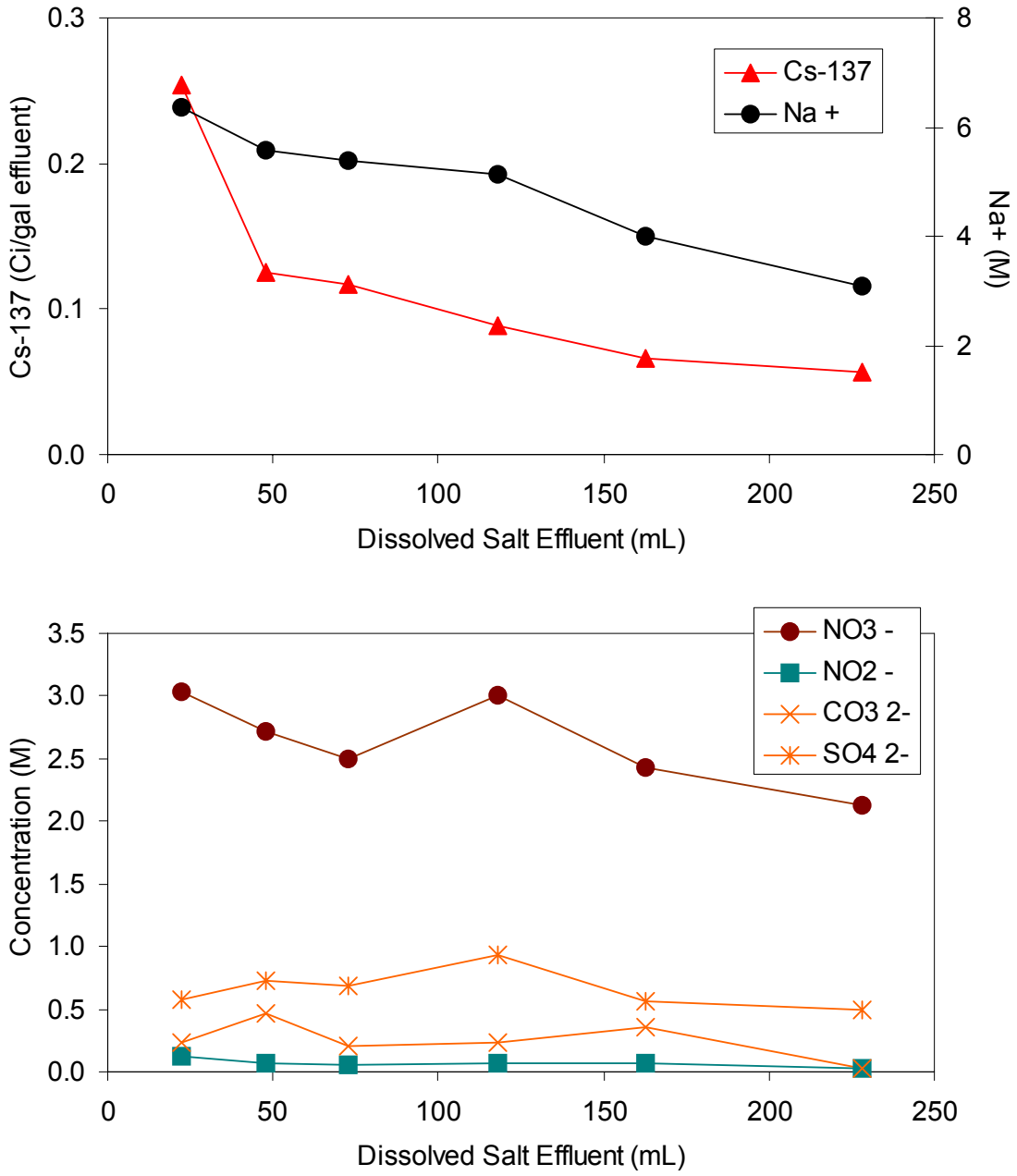

Figure 9: Tank 10H sample HTF-609 flow-through dissolution profiles for ^{137}Cs and Na^{+} (top), and anions (bottom)

Comparison of Components and Streams

Table 5, Table 6, and Table 7 contain summaries of the radiological, ionic, and elemental composition, respectively, of the undrained saltcake, the filtered interstitial liquid (IL), and the drained/dissolved saltcake (DDS). The characterization results for both the solid and the liquid streams are presented in per mass units to ease comparison and calculation. The tables are compilations of results from several separate preparations and analytical methods.

The right-most column of Table 5 through Table 7, labeled “Partition into IL (%)”, is an estimate for each component of the percentage measured in the undrained saltcake that was contained in the interstitial liquid residing in the saltcake pores. Subtracting the Partition into IL (PIL) from 100% yields an estimate for each component of the percentage contained in the solid phase of the original saltcake sample.

Compared to other tanks, the calculation of the partitioning of components into the interstitial liquid differed for this Tank 10H analysis. For previous samples, the PIL for each component was calculated by the wt % of the component measured in the filtered IL multiplied by the wt % of IL in the undrained saltcake and divided by the wt % of the component measured in the undrained saltcake. For Tank 10, however, new values for the wt % liquid in the undrained saltcake were calculated so that the partition into IL for ^{137}Cs would equal 100%. These adjusted water contents for the undrained bulk saltcake samples are contained in Table 3, labeled “(adj)”. If the original wt % liquid in the undrained saltcake values are used, labeled “(mes)” in Table 3, the calculated values for ^{137}Cs PIL would be 149% for HTF-610 and 61% for HTF-611. If the water content measurement was not the true cause of the partitioning discrepancy in HTF-610, the cause was likely the intra-sample heterogeneity of the IL. Although it does not affect the conclusions, the PIL for undrained saltcake from HTF-610 used the composition of IL from HTF-610, while the calculation for saltcake from HTF-611 used the composition of IL from HTF-609.

Based on the adjusted water content, the PIL for many components is statistically indistinguishable from 100%, including nitrite, hydroxide, and aluminate. Some components, conversely, are present in the interstitial liquid at much lower levels than in the saltcake solids, including uranium, plutonium, strontium, thorium, americium, sulfate, oxalate, and most metals (silver, barium, calcium, copper, iron, manganese, nickel, and silicon). Several other components appear to be contained in both the interstitial liquid and the saltcake solids, including technetium, sodium, nitrate, carbonate, and chromium. These results are consistent with other saltcake samples, with the exception of the larger insoluble fraction of technetium in HTF-610.[6] It is expected that the insoluble technetium is associated with the insoluble, sludge-like solids.

Table 6 contains several values that are calculated from multiple analytical techniques. The mass balance for each stream is calculated by summing the analytes in Table 6 that are above detection limits and the adjusted water content in Table 3. In the case of the drained/dissolved saltcake from HTF-609, the water content information was unknown. The mass balance was set to 100% to estimate the free liquid (FL) water content reported in Table 3. The charge balance for each stream is calculated by summing the normalities of the anions and dividing by the sum of the normalities of the cations. Charge balance values above 100% indicate that more anions were measured than would correspond to the cation measurement. The calculated hydroxide concentration is used to check the measured free hydroxide titration. It estimates the free hydroxide by taking the total base measured by titration and subtracting the carbonate by TIC and the aluminate by ICP-ES. Total cesium is calculated as the sum of ^{133}Cs by ICP-MS and the ^{137}Cs from radiochemistry. Several other components, phosphate, sulfate, and potassium, have been measured by two equally valid methods, and both are shown in Table 6.

Sulfate and phosphate measured independently by ICP-ES and IC are in good agreement in most cases. The calculated estimate of free hydroxide is near the measured value for most cases.

Table 8 compares the liquid stream compositions which are projected to be encountered during tank waste retrieval. The IL drained from samples HTF-609 and HTF-610 (converted to molarity from the values in the previous summary tables) would be similar to the material that will be removed during draining. Although there is a good match between the compositions of the two interstitial liquid samples, the interstitial liquid may not be representative of that from lower tank elevations.

Table 8 contains the direct measurement for the filtered drained dissolved salt (DDS) from the bottom of sample HTF-609 at 4.35 M [Na^+] and calculated values for the adjusted drained dissolved salt stream (ADDS) (i.e., mathematically adjusted to 6.0 M [Na^+]). Note that, while the directly measured DDS stream was filtered and thus contained no insoluble solids, it was likely undersaturated with

respect to salt components expected during salt dissolution. The ADDS stream, however, was calculated from a stream of lower salt composition and thus may overestimate the concentrations of some sparingly soluble species since equilibrium saturation is not considered.

Of interest is the comparison of the interstitial liquid and drained/dissolved salt for HTF-609. Because Tank 10H has undergone previous salt removal via dissolution, the IL in the Tank 10H samples has a higher nitrate and a lower nitrite and hydroxide composition than would be expected based on previous tank analysis.[6] Even so, the compositions of the DDS is very different than the IL, with the IL being a saturated solution with high hydroxide (9.5 M [Na^+], 3.6 M [OH^-]) to the DDS being an unsaturated solution with low hydroxide (4.35 M [Na^+], 0.13 M [OH^-]).

The other streams contained in Table 8 are, for samples HTF-610 and HTF-611, the calculated undrained dissolved salt (UDS-0) and the prediction for the drained dissolved salt calculated with removal of 25%, 50%, and 100% of the interstitial liquid (DDS-25, DDS-50, and DDS-100, respectively). Again, the interstitial liquid composition for HTF-610 was taken as that of the IL drained from HTF-610, and for that for HTF-611 was taken as the IL drained form HTF-609. The undrained dissolved salt and the predicted drained dissolved salt streams are compared at a total sodium concentration of 6 M. These 6 M streams do not account for the solubility of the individual components in the saltcake. The values for these dissolved salt streams includes the contribution from the solids that may be present, which would include some less soluble salts and water insoluble solids. The dissolved salt streams are average values for the complete dissolution (or slurrying) of the saltcake and do not account for selective or sequential dissolution. During dissolution processes occurring over several stages with liquid movement within the saltcake, the more soluble components, such as OH^-, NO_2^-, and ^{137}Cs, would be more concentrated in earlier stages while less soluble components, such as CO_3^{2-}, SO_4^{2-}, ^{90}Sr, and other sludge components would be more concentrated in the later stages.[7]

Using Table 8, the adjusted drained/dissolved salt stream (ADDS) from HTF-609 can be compared with the 50% drained dissolved salt predictions from HTF-610 and HTF-611 (DDS-50). All three of these 6 M [Na^+] dissolved salt streams contain approximately the same concentration of the most soluble components (cesium, hydroxide, nitrite and aluminate). The HTF-610 stream has a much larger content of ^{90}Sr, sulfate, and carbonate and a much smaller nitrate than does the HTF-611 stream. The HTF-609 ADDS stream has nitrate, sulfate, and carbonate composition that is intermediate to the two other streams (DDS-50 from HTF-610 and HTF-611).

Also included in Table 8 are values for each stream indicating the grams of salt required to produce a 6 M [Na^+] solution. Finally, Table 8 contains an estimate of the amount of sludge projected present in the dissolved salt solutions, based on the concentration of metals in the saltcake. This estimate does not contain mass contributions by silicon, aluminum, and radionuclides. The composition of the sludge in HTF-610 was approximately 93 wt % $Fe(OH)_3$, 3 wt % HgO, 2 wt % MnO_2, 1 wt % $Cr(OH)_3$, and <1 wt % of several other components($Ni(OH)_2$, $BaSO_4$, and AgOH). The composition of the sludge in HTF-611 was approximately 84 wt % $Fe(OH)_3$, 13 wt % HgO, and 4 wt % $Cr(OH)_3$. The analyzed portion of HTF-610 contained considerable sludge solids (nearly 1 wt %) by comparison with typical saltcake. Both Tank 10H samples had high levels of mercury when compared with other recent saltcake samples.

Figure 10 and appendix Table 24 indicate the likely composition of the solid phase in the original undrained sample, formulated from the major components of saltcake after IL removal (similar calculation as DDS-100). Finally, the saltcake composition is normalized to sum to 100 wt%. The un-normalized composition of the solid phase of HTF-610 and HTF-611 were slightly larger than 100 wt %; 102 and 105 wt % respectively. Both HTF-610 and HTF-611 have carbonates and sulfates contributing to the solid phase. HTF-610, however, has a uniquely large percentage of carbonates and sulfates, with sodium nitrate contributing only 35 wt % of the solid phase. It is likely that this concentrated layer of sulfates and carbonates is remnant from the previous Tank 10H dissolution, where interstitial liquid and sodium nitrate were removed. Leaving the less soluble salts, ^{90}Sr, and actinides that settled into a layer. The deeper sample, HTF-611, is a more typically observed sodium nitrate salt mixture.

Table 5: Summary of Radiological Composition of Tank 10H Samples

Analyte	Units	Method	HTF-609		HTF-610				HTF-611		
			IL (filtered)	DDS (filtered)	undrained saltcake		IL (filtered)	Partition Into IL (%)	undrained saltcake		Partition Into IL (%)
					average	stdev			average	stdev	
^{14}C	pCi/g	Rad. Chem.	--	--	2.2E+04	--	--	--	--	--	--
^{90}Sr	pCi/g	Rad. Chem.	1.67E+04	6.56E+04	5.36E+07	6.4E+06	--	0.005	1.43E+06	1.2E+05	0.2
^{99}Tc	pCi/g	ICP-MS	1.04E+05	4.69E+03	4.93E+04	2.8E+03	1.48E+05	50	2.14E+04	5.1E+02	66
^{135}Cs	pCi/g	ICP-MS	2.20E+03	8.86E+01	5.46E+02	5.7E+01	2.94E+03	90	3.31E+02	1.7E+01	91
^{137}Cs	pCi/g	Rad. Chem.	6.13E+08	2.13E+07	1.14E+08	9E+06	6.80E+08	100*	8.36E+07	3.4E+06	100*
^{230}Th	pCi/g	ICP-MS	< 1.9E+03	< 3.0E+02	< 3.2E+03	--	< 9.9E+02	5	< 3.2E+03	--	--
^{232}Th	pCi/g	ICP-MS	< 1.0E-02	< 1.5E-03	2.09E+00	2.9E-01	< 5.1E-03	< 0.04	< 1.7E-02	--	--
^{233}U	pCi/g	ICP-MS	< 8.9E+02	< 1.4E+02	9.1E+03	1.7E+03	< 4.5E+02	< 1	3.8E+03	5E+02	< 3
^{234}U	pCi/g	ICP-MS	< 5.8E+02	< 8.8E+01	1.9E+03	2E+02	< 2.9E+02	< 3	1.2E+03	2E+02	< 7
^{235}U	pCi/g	ICP-MS	2.7E-01	5.4E-02	1.35E+01	1.8E+00	3.0E-01	0.4	1.11E+01	1E-01	0.3
^{236}U	pCi/g	ICP-MS	< 6.0E+00	< 9.1E-01	1.24E+02	1.6E+01	3E+00	0.4	9.24E+01	5.3E+00	0.9
^{237}Np	pCi/g	ICP-MS	< 6.5E+01	< 9.9E+00	5.2E+02	2.0E+02	< 3.3E+01	< 1	1.6E+02	5E+01	< 5
^{238}U	pCi/g	ICP-MS	2.82E-01	7.42E-02	2.84E+01	4.0E+00	2.90E-01	0.2	5.15E+00	4.7E-01	0.7
^{238}Pu	pCi/g	Rad. Chem.	1.64E+04	3.87E+03	1.27E+06	1.6E+05	1.03E+04	0.1	9.86E+04	7.1E+03	2
$^{239/240}Pu$	pCi/g	Rad. Chem.	1.84E+03	3.07E+02	1.77E+04	1.6E+03	2.47E+03	2	5.4E+03	4.9E+03	5
^{239}Pu	pCi/g	ICP-MS	< 5.7E+03	< 8.8E+02	1.3E+04	5.7E+02	< 2.9E+03	< 4	< 9.4E+03	--	--
^{240}Pu	pCi/g	ICP-MS	< 2.1E+04	< 3.2E+03	< 3.4E+04	--	< 1.1E+04	--	< 3.4E+04	--	--
^{241}Pu	pCi/g	ICP-MS	< 9.5E+06	< 1.5E+06	< 1.5E+07	--	< 4.8E+06	--	< 1.6E+07	--	--
^{241}Am	pCi/g	Rad. Chem.	< 9.89E+02	1.68E+02	2.35E+04	1.18E+04	< 7.66E+02	< 0.5	1.44E+03	4.1E+02	< 9
^{242}Pu	pCi/g	ICP-MS	< 3.5E+02	< 5.4E+01	< 5.7E+02	--	< 1.8E+02	--	< 5.8E+02	--	--
Uranium Summary											
Total U	wt %	ICP-MS	9.67E-05	2.46E-05	9.40E-03	1.32E-03	1.05E-04	0.2	2.25E-03	1.5E-04	0.6
^{235}U Enrichment	wt %	ICP-MS	13.1%	10.3%	6.63%	0.03%	14.0%	--	23.0%	1.4%	--

*based on adjusted water contents; equates to fixing ^{137}Cs PIL as equal to 100%

Table 6: Summary of Ionic Composition of Tank 10H Samples

Analyte	Units	Method	HTF-609		HTF-610				HTF-611		
			IL (filtered)	DDS (filtered)	undrained saltcake		IL (filtered)	Partition Into IL (%)	undrained saltcake		Partition Into IL (%)
					average	stdev			average	stdev	
Na^+	wt %	ICP-ES	1.52E+01	8.14E+00	2.84E+01	2.0E+00	1.50E+01	9	2.58E+01	4E-01	8
NO_3^-	wt %	IC	1.47E+01	1.11E+01	2.38E+01	2.2E+00	1.41E+01	10	6.40E+01	1.8E+00	3
NO_2^-	wt %	IC	4.76E+00	2.19E-01	9.43E-01	2.83E-01	7.74E+00	138	9.13E-01	2.47E-01	71
OH^-	wt %	Wet Chem.	4.20E+00	1.81E-01	7.30E-01	1.89E-01	3.45E+00	79	4.94E-01	4.9E-02	116
OH^-	wt %	Calculated	3.23E+00	--	2.49E+00	1.0E-01	4.94E+00	33	3.07E-01	1.45E-01	144
AlO_2^-	wt %	ICP-ES	2.86E+00	9.60E-02	6.24E-01	6.5E-02	3.67E+00	99	4.46E-01	1.1E-02	87
CO_3^{2-}	wt %	TIC/TOC	1.50E+00	1.83E+00	1.17E+01	6E-01	5.73E-01	1	1.46E+00	8E-03	14
SO_4^{2-}	wt %	IC	3.78E-01	4.09E+00	2.35E+01	3.6E+00	2.66E-01	0.2	2.36E+00	6.2E-01	2
SO_4^{2-}	wt %	ICP-ES	5.19E-01	4.35E+00	2.35E+01	2.4E+00	4.13E-01	0.3	2.06E+00	7E-02	3
PO_4^{3-}	wt %	IC	1.40E-01	</=1.67E-02	< 5.01E-01	--	1.42E-01	> 5	< 4.89E-01	--	> 4
PO_4^{3-}	wt %	ICP-ES	1.60E-01	< 2.59E-02	</=9.53E-02	1.94E-02	1.38E-01	> 24	< 7.97E-02	--	> 27
Cl^-	wt %	IC	</=1.30E-02	< 4.45E-03	< 1.00E-01	--	< 6.48E-03	--	< 9.77E-02	--	--
F^-	wt %	IC	< 1.30E-02	< 4.45E-03	< 1.00E-01	--	< 6.48E-03	--	< 9.77E-02	--	--
$C_2O_4^{2-}$	wt %	IC	< 6.51E-02	</=1.67E-02	1.42E-01	3.6E-02	< 3.24E-02	4	3.66E-01	7.3E-02	2
CHO_2^-	wt %	IC	< 6.51E-02	< 2.22E-02	< 5.01E-01	--	< 3.24E-02	--	< 4.89E-01	--	--
K^+	wt %	AA	--	--	1.98E-02	1.9E-03	--	--	1.43E-02	3E-04	--
K^+	wt %	ICP-ES	< 6.22E-01	</=2.36E-02	< 5.07E-01	--	1.16E-01	--	< 5.10E-01	--	--
Cs^+	wt %	ICP-MS/RdChm	2.13E-03	8.18E-05	4.43E-04	2.1E-05	2.79E-03	105	3.05E-04	5E-06	95
TOC	wt %	TIC/TOC	1.3E-01	--	4.5E-01	5E-02	2.80E-01	11	1.9E-01	2E-02	9
Mass Balance	%	Calculated	97	26 + water	99		97	--	100		--
Charge Bal (-/+)	%	Calculated	106	97	110		106	--	108		--

Table 7: Summary of Other Elemental Composition of Tank 10H Samples

Analyte	Units	Method	HTF-609		HTF-610				HTF-611		
			IL (filtered)	DDS (filtered)	undrained saltcake		IL (filtered)	Partition Into IL (%)	undrained saltcake		Partition Into IL (%)
					average	stdev			average	stdev	
Ag	wt %	ICP-ES	< 9.80E-04	< 8.06E-05	1.43E-03	2.7E-04	< 2.68E-04	< 3	< 8.04E-04	--	--
As	wt %	AA	--	--	< 2.66E-04	--	--	--	< 2.68E-04	--	--
B	wt %	ICP-ES	< 1.06E-01	< 1.33E-03	< 8.63E-02	--	< 4.43E-03	--	< 8.68E-02	--	--
Ba	wt %	ICP-ES	< 9.80E-04	1.27E-04	1.23E-03	3.1E-04	4.17E-04	6	< 8.04E-04	--	--
Ca	wt %	ICP-ES	< 2.96E-02	6.85E-04	</=2.65E-02	3.4E-03	8.61E-04	< 1	< 2.43E-02	--	--
Cd	wt %	ICP-ES	< 1.31E-03	< 2.42E-04	< 1.06E-03	--	< 8.05E-04	--	< 1.07E-03	--	--
Ce	wt %	ICP-ES	< 1.62E-02	2.06E-03	< 1.32E-02	--	4.61E-03	> 6	< 1.33E-02	--	--
Co	wt %	ICP-MS	2.19E-05	9.05E-06	9.0E-05	6.1E-05	3.46E-05	6	< 1.4E-05	--	> 22
Cr	wt %	ICP-ES	8.40E-03	< 8.06E-04	9.44E-03	7.43E-03	8.33E-03	15	1.15E-03	1.4E-04	100
Cu	wt %	ICP-ES	< 2.03E-03	< 2.02E-04	</=1.85E-03	2.8E-04	< 6.71E-04	< 6	< 1.66E-03	--	--
Fe	wt %	ICP-ES	< 1.44E-03	< 1.61E-04	8.99E-01	3.12E-01	< 5.37E-04	< 0.01	1.53E-02	3.9E-03	< 1
Gd	wt %	ICP-ES	< 1.76E-03	2.35E-04	< 1.44E-03	--	5.45E-04	> 6	< 1.45E-03	--	--
Hg	wt %	CV AA	--	--	5.03E-02	4E-04	--	--	4.07E-03	7E-05	--
La	wt %	ICP-ES	< 1.31E-03	2.73E-04	< 1.06E-03	--	< 6.04E-04	--	< 1.07E-03	--	--
Li	wt %	ICP-ES	< 5.56E-03	6.98E-04	< 4.53E-03	--	1.46E-03	> 5	< 4.55E-03	--	--
Mg	wt %	ICP-ES	< 4.05E-03	< 4.03E-05	< 3.30E-03	--	< 1.34E-04	--	< 3.32E-03	--	--
Mn	wt %	ICP-ES	< 1.44E-03	< 6.05E-05	2.88E-02	5.7E-03	< 2.01E-04	< 0.1	< 1.18E-03	--	--
Mo	wt %	ICP-ES	< 1.33E-02	< 1.35E-03	< 1.09E-02	--	7.35E-03	> 11	< 1.09E-02	--	--
Ni	wt %	ICP-ES	< 4.90E-03	< 9.07E-04	</=6.07E-03	3.30E-03	< 3.02E-03	< 8	< 4.02E-03	--	--
Pb	wt %	ICP-ES	< 1.61E-02	< 5.76E-03	< 1.31E-02	--	< 1.92E-02	--	< 1.32E-02	--	--
Sb	wt %	ICP-ES	< 9.87E-03	< 1.43E-03	< 8.04E-03	--	5.24E-03	> 11	< 8.09E-03	--	--
Se	wt %	AA	--	--	3.51E-04	4.3E-05	--	--	< 2.68E-04	--	--
Si	wt %	ICP-ES	< 2.42E-03	< 5.04E-04	4.43E-02	1.15E-02	< 1.68E-03	< 1	6.70E-03	5.9E-04	< 5
Sn	wt %	ICP-ES	< 1.60E-02	< 2.30E-03	</=1.38E-02	1.3E-03	< 7.65E-03	--	< 1.31E-02	--	--
Sr	wt %	ICP-ES	< 6.54E-03	< 1.61E-04	</=5.79E-03	6.9E-04	< 5.37E-04	--	< 5.36E-03	--	--
Ti	wt %	ICP-ES	< 3.92E-04	< 2.62E-04	7.98E-04	2.53E-04	< 8.72E-04	< 18	3.21E-04	2.1E-05	< 17
V	wt %	ICP-ES	< 7.19E-04	< 2.22E-04	< 5.86E-04	--	8.47E-04	> 24	< 5.89E-04	--	--
Zn	wt %	ICP-ES	7.35E-02	3.62E-03	1.53E-02	1.4E-03	5.29E-02	58	4.09E-03	2.2E-04	245
Zr	wt %	ICP-ES	< 7.84E-04	< 2.82E-04	</=6.54E-04	8.1E-05	< 9.40E-04	< 24	< 6.43E-04	--	--

Table 8: Stream Composition Projections for Draining and Dissolution of Tank 10H Saltcake

Analyte	Units	Method	HTF-609			HTF-610					HTF-611			
			IL	DDS	ADDS	IL	UDS-0	DDS-25*	DDS-50*	DDS-100*	UDS-0	DDS-25*	DDS-50*	DDS-100*
Na^+	M	ICP-ES	9.49	4.35	6.00	9.38	6.00	6.00	6.00	6.00	6.00	6.00	6.00	6.00
NO_3^-	M	IC	3.39	2.21	3.05	3.27	1.87	1.87	1.86	1.85	5.52	5.58	5.66	5.81
NO_2^-	M	IC	1.48	0.059	0.081	2.42	0.100	0.067	0.033	0	0.106	0.089	0.071	0.033
OH^-	M	Wet Chem.	3.55	0.131	0.180	2.91	0.209	0.171	0.132	0.048	0.155	0.113	0.068	0
OH^-	M	Calculated	2.73	--	--	4.18	0.713	0.668	0.621	0.522	0.096	0.063	0.028	0
AlO_2^-	M	ICP-ES	0.695	0.0200	0.0276	0.895	0.0515	0.0397	0.0273	0.0008	0.0404	0.0322	0.0237	0.0055
CO_3^{2-}	M	TIC/TOC	0.360	0.375	0.517	0.137	0.952	0.971	0.992	1.04	0.130	0.128	0.126	0.121
SO_4^{2-}	M	IC	0.0564	0.524	0.722	0.0397	1.19	1.22	1.25	1.30	0.131	0.133	0.135	0.140
SO_4^{2-}	M	ICP-ES	0.0776	0.558	0.769	0.0619	1.19	1.22	1.24	1.30	0.115	0.116	0.118	0.121
PO_4^{3-}	M	IC	0.0212	<=0.0022	<=0.0030	0.0216	<0.0256	--	--	--	<0.0275	--	--	--
PO_4^{3-}	M	ICP-ES	0.0242	<0.0034	<0.0046	0.0209	<=0.0049	--	--	--	<0.0045	--	--	--
Cl^-	M	IC	<=0.0053	<0.0015	<0.0021	<0.0026	<0.0137	--	--	--	<0.0147	--	--	--
F^-	M	IC	<0.0098	<0.0029	<0.0040	<0.0049	<0.0256	--	--	--	<0.0275	--	--	--
$C_2O_4^{2-}$	M	IC	<0.0106	<=0.0023	<=0.0032	<0.0053	0.0078	--	--	--	0.0222	--	--	--
CHO_2^-	M	IC	<0.0208	<0.0061	<0.0084	<0.0103	<0.0541	--	--	--	<0.0580	--	--	--
K^+	M	AA	--	--	--	--	0.0025	--	--	--	0.0020	--	--	--
K^+	M	ICP-ES	<0.228	<=0.0074	<=0.0102	0.0427	<0.0631	--	--	--	<0.0698	--	--	--
Cs^+	mM	ICP-MS/RdChm	0.227	0.0075	0.0103	0.297	0.0160	0.0120	0.0079	0	0.0121	0.0094	0.0066	0.0006
^{90}Sr	pCi/mL	Rad. Chem.	2.40E+04	8.07E+04	1.11E+05	--	2.61E+07	2.67E+07	2.73E+07	2.86E+07	7.65E+05	7.80E+05	7.96E+05	8.31E+05
^{137}Cs	pCi/mL	Rad. Chem.	8.79E+08	2.62E+07	3.61E+07	9.78E+08	5.55E+07	4.26E+07	2.90E+07	0	4.47E+07	3.42E+07	2.33E+07	8.66E-09
^{238}Pu	pCi/mL	Rad. Chem.	2.35E+04	4.76E+03	6.56E+03	1.48E+04	6.20E+05	6.34E+05	6.48E+05	6.79E+05	5.27E+04	5.35E+04	5.43E+04	5.61E+04
sludge	mg/L	ICP-ES	--	--	--	--	9006	9205	9413	9861	193	193	193	194
g salt / L 6M Na^+			--	--	--	--	486	476	466	444	535	527	519	502

* Drained Dissolved Salt solutions calculated by removing a percentage (25%, 50%, or 100%) of the IL

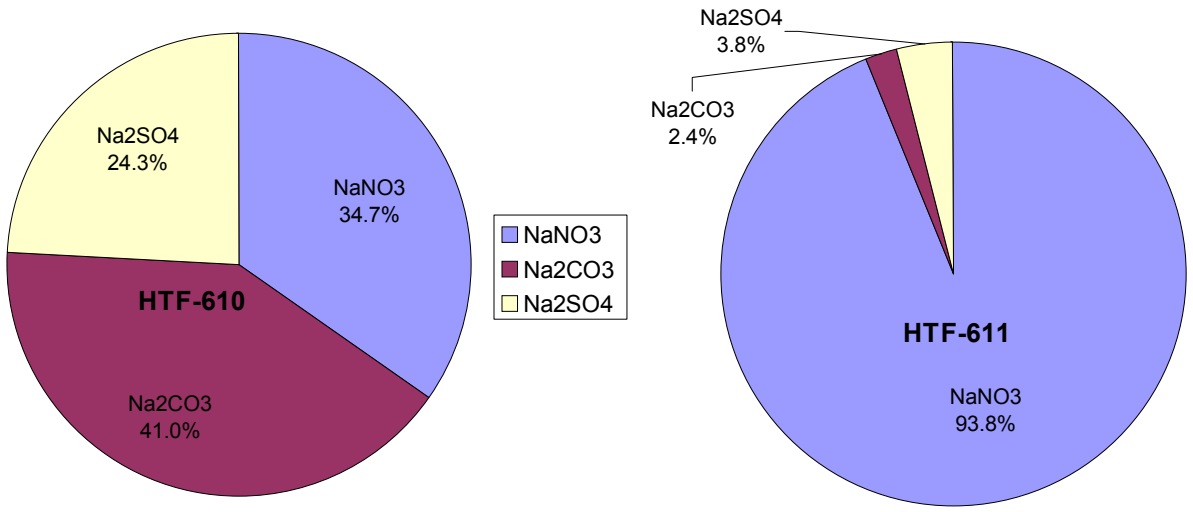

Figure 10: Likely major components of Tank 10H salt solids, normalized.

Hydraulic Properties

Draining

Figure 11 contains the temporal draining observations for two of the Tank 10H samples (HTF-609 and HTF-610). The interstitial liquid drained out of sample HTF-609 much faster than it did out of HTF-610. This correlates with the microscopic salt characteristics noted later in this report. Analysis of results from SEM of salt samples revealed that the top of sample HTF-609 had large, loose, distinct grains and the top of sample HTF-610 appeared to be more consolidated and have more fine grained precipitates covering and perhaps cementing large grains together. As displayed in Figure 12, post drainage water content analyses of samples from the top and bottom of HTF-609 show that the top of the sample was drier than the bottom of the sample, while the water content in HTF-610 appears to be more uniform. These results suggest that there is a transition from coarser grained salt to finer grained salt within sample HTF-609, which would result in a water content profile similar to that shown in Figure 12. Likewise, the slower drainage and more uniform water in sample HTF-610 suggests a smaller more uniform grain size within the sample.

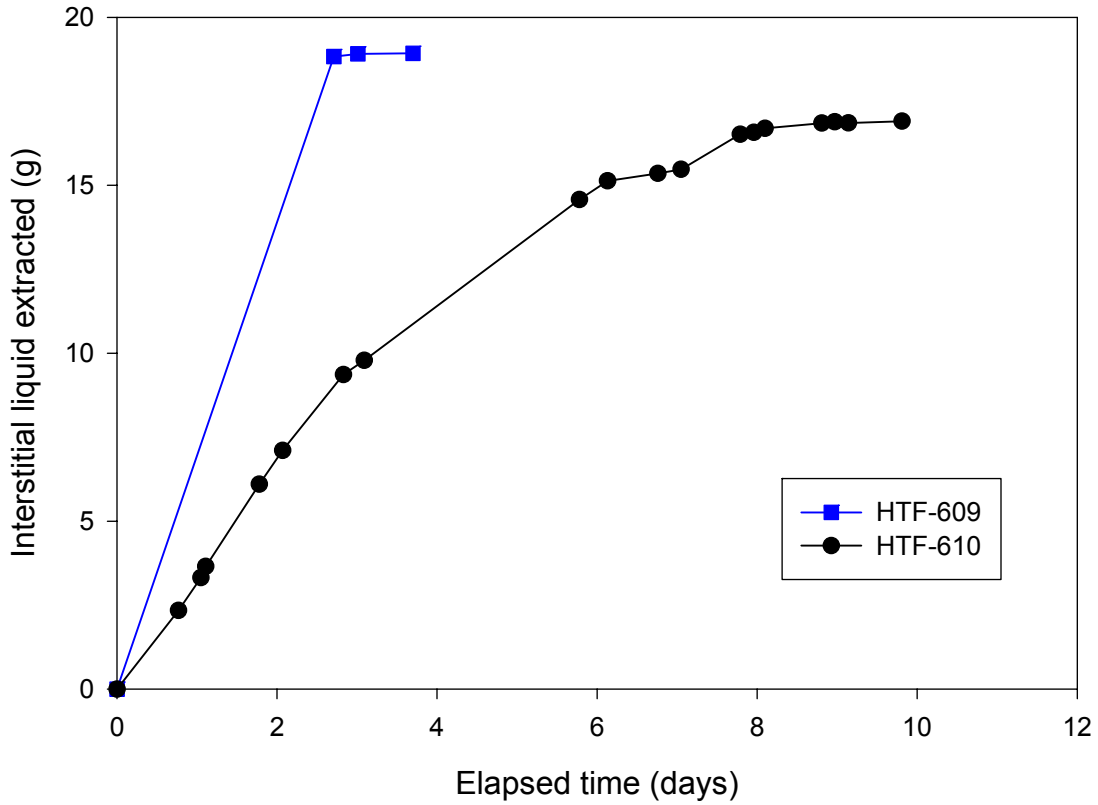

Figure 11: Draining behavior of the Tank 10H saltcake samples

Based on the conceptual model for drainage with sandy loam as a porous media analog,[8] the average saturation after drainage of Tank 10H would occur at a vacuum 1.9 in. Hg. A schematic of the calculated in-tank draining of Tank 10H is shown in Figure 13. Considerably more vacuum was applied (8 in. Hg in test) in the laboratory draining of the Tank 10H samples than is attainable by gravity draining in Tank 10H (1.9 in. Hg in tank). This difference was necessitated by the desire to draw sufficient vacuum to extract some fluid for analysis.

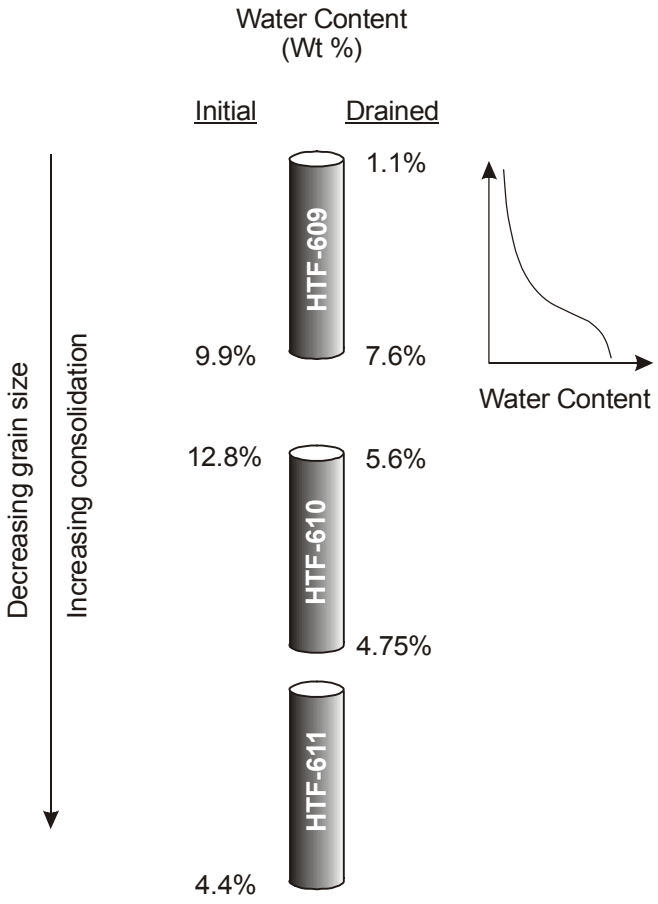

Figure 12: Water content of as-received and drained Tank 10H samples.

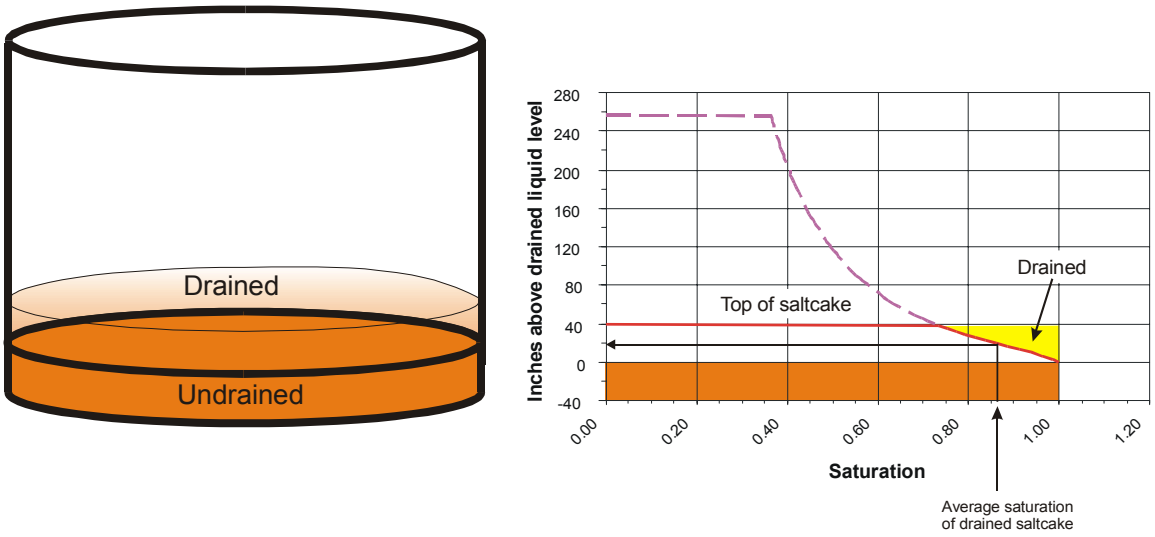

Figure 13: Theoretical drainage curve for salt cake in Tank 10H with the top of salt at 78 inches, final liquid level in caisson of 40 inches, and sandy loam drainage curve.

Saltcake Hydraulic Conductivity and Permeability

Falling-head tests were conducted on sample HTF-609 over a 2 day period from November 20 – 21, 2003. Five measurements of hydraulic conductivity were conducted on each day. Table 9 contains the details of the hydraulic conductivity measurements. The first 5 hydraulic conductivity measurements reported in Table 9 are from the first day of testing and are more representative of the as-received saltcake. The average hydraulic conductivity from the first day of testing is $4.2 * 10^{-4}$ cm/sec, which is similar to that for a fine to medium grained sand.

Table 9: Hydraulic conductivity of saltcake samples from Tank 10H.

#	Delta T (min)	A (cm^2)	a (cm^2)	l (cm)	ho (cm)	ht (cm)	K SIL @ 18C (cm/sec)
1	2040	4.57	1.1	15.24	15.3	12.608	3.50E-04
2	3660	4.57	1.1	15.24	11.0	7.745	3.53E-04
3	4200	4.57	1.1	15.24	7.7	4.955	3.92E-04
4	4680	4.57	1.1	15.24	11.0	6.071	4.68E-04
5	1800	4.57	1.1	15.24	11.0	8.396	5.53E-04
6	3540	4.57	1.1	15.24	11.0	4.397	9.54E-04
7	1860	4.57	1.1	15.24	11.0	6.5825	1.02E-03
8	1080	4.57	1.1	15.24	11.0	5.885	2.13E-03
9	900	4.57	1.1	15.24	11.0	6.536	2.13E-03
10	360	4.57	1.1	15.24	11.0	8.8145	2.27E-03

The flow of Simulated Interstitial Liquid (SIL) through the sample was stopped at the end of the first day of testing and was resumed on the second day of testing, allowing the SIL to sit in the sample overnight. During the test, a total of 56.8 ml of SIL was passed through the sample. Figure 14 contains the trend in hydraulic conductivity measurements over the course of the test. On the first day, 19.2 mL of SIL (slightly more than the estimated pore volume of 18.3) flowed through the column and the hydraulic conductivity was relatively stable, increasing about 40% over the course of the day. The hydraulic conductivity increased throughout the second day of testing as a total of nearly three pore volumes flowed through the sample, resulting in an over 500% increase over the hydraulic conductivity measured on the first day.

The increase in hydraulic conductivity may be the result of changing fluid properties due to mixing of SIL with residual IL. Likewise, interactions between the SIL and saltcake (dissolution and/or precipitation of salts) may have increased the permeability over the course of the testing. Because of the previous dissolution history of Tank 10H, the IL within the samples was weighted towards higher nitrate and lower nitrite and hydroxide than is typical of IL from other samples. The SIL recipe, as seen in Table 2, was based on previous IL samples, and thus had a composition that deviated from that of the actual Tank 10H IL.

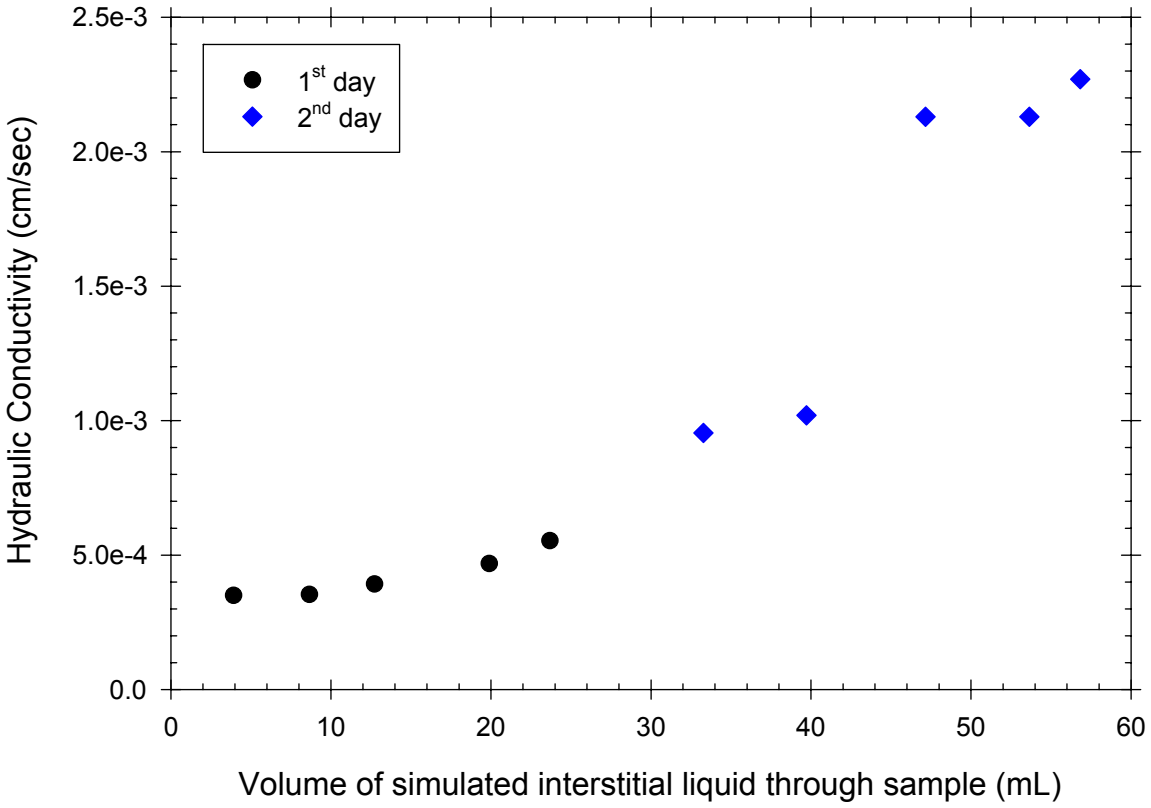

Figure 14: Hydraulic conductivity during falling head testing of sample HTF-609 from Tank 10H

Interstitial Liquid Displacement – Washing

Previous reports have suggested that the radioactive cesium could be "washed" from the salt through a process called interstitial liquid displacement (ILD), in which a non-radioactive fluid of similar composition to the IL is forced through the saltcake.[9,10] Although this concept has obstacles that hinder full-tank implementation, it was readily demonstrated on a one-foot-long core sample from Tank 41H.[5] While performing hydraulic conductivity testing on the Tank 10H sample, samples of the column effluent were taken periodically to replicate the results of the previous ILD test.

As with Tank 41H, the flow of SIL through Tank 10H sample HTF-609 removed ^{137}Cs and other ions present in residual IL. Table 10 and Figure 15 contain results from the ICP-ES and gamma spec. analysis for ^{137}Cs versus the volume of SIL passed through the sample (and versus the calculated interstitial porous volume). The full set of data from the washing analyses is available in the appendix in Table 25. The processes responsible for removal of aluminum from the sample are similar to those for ^{137}Cs and ^{99}Tc as shown in Figure 16, which indicates that the Al recovered during the test came primarily from residual IL and not from the dissolution of Al salts in the sample. Sodium concentration in the effluent steadily increased from 10.05 to 10.5 M during the test and did not reach the SIL concentration of 10.8 molar. Although still within the analytical uncertainty, this behavior is further evidence of SIL/IL and SIL/salt interactions during hydraulic conductivity and ILD tests.

Table 10: Selected analytical results for samples collected during the falling head test on sample HTF-609.

Cumulative Volume Through Sample (mL)	Cumulative Number of Pore Volumes	$[Na^+]$ (M)	$[AlO_2^-]$ (M)	$[SO_4^{2-}]$ (M)	^{137}Cs (Ci/gal)	^{99}Tc (pCi/mL)
3.15	0.16	10.05	0.15	0.04	8.19E-01	4.33E+04
7.05	0.36	10.29	0.13	0.03	6.99E-01	3.68E+04
10.1	0.52	10.29	0.11	0.04	6.25E-01	3.32E+04
19.15	0.98	10.47	0.08	0.03	4.25E-01	2.28E+04
36.27	1.86	10.41	0.04	0.03	2.05E-01	1.08E+04
56.82	2.91	10.47	0.01	0.03	7.04E-02	4.12E+03
IL	--	9.49	0.69	0.06	3.33	1.48E+05
SIL	--	10.8	a	a	a	a

a = not included in simulated interstitial liquid

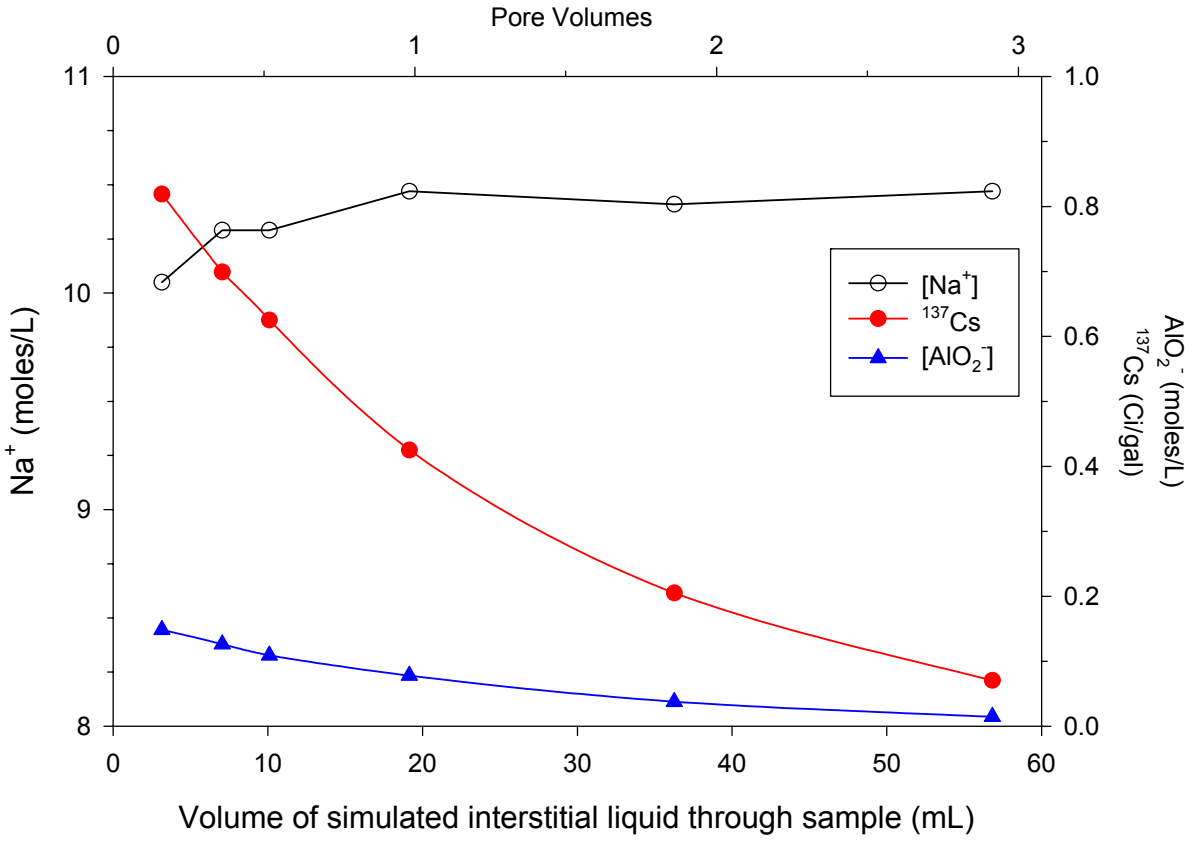

Figure 15: ^{137}Cs and specific ion concentrations in effluent from falling-head test on HTF-609.

An estimated 91% of the residual ^{137}Cs in the drained salt sample HTF-609 was removed by 2.9 pore volumes of SIL during the falling head permeability test. During the Tank 41H ILD test, 97% of the ^{137}Cs was removed by 2.5 pore volumes of SIL. The higher hydraulic conductivity in the Tank 10H sample resulted in faster flow than in the Tank 41H sample for similar test conditions. This decreased the amount of time for diffusion of ^{137}Cs from residual IL into the SIL and may have lowered the "efficiency" of ^{137}Cs removal. Using an initial ^{137}Cs inventory estimated from the ^{137}Cs removal model in Figure 17 and results from IL analysis, the water content of the drained sample is estimated to be 2.7 wt %, which is consistent with the conceptual draining model for sample HTF-609 shown in Figure 12. The residual ^{137}Cs was not measured in the washed Tank 10H sample.

Many sparingly soluble species had low but constant concentrations in the effluent. The actinides U and Pu, as well as barium and iron, had constant or even slightly increasing concentrations throughout the washing process.

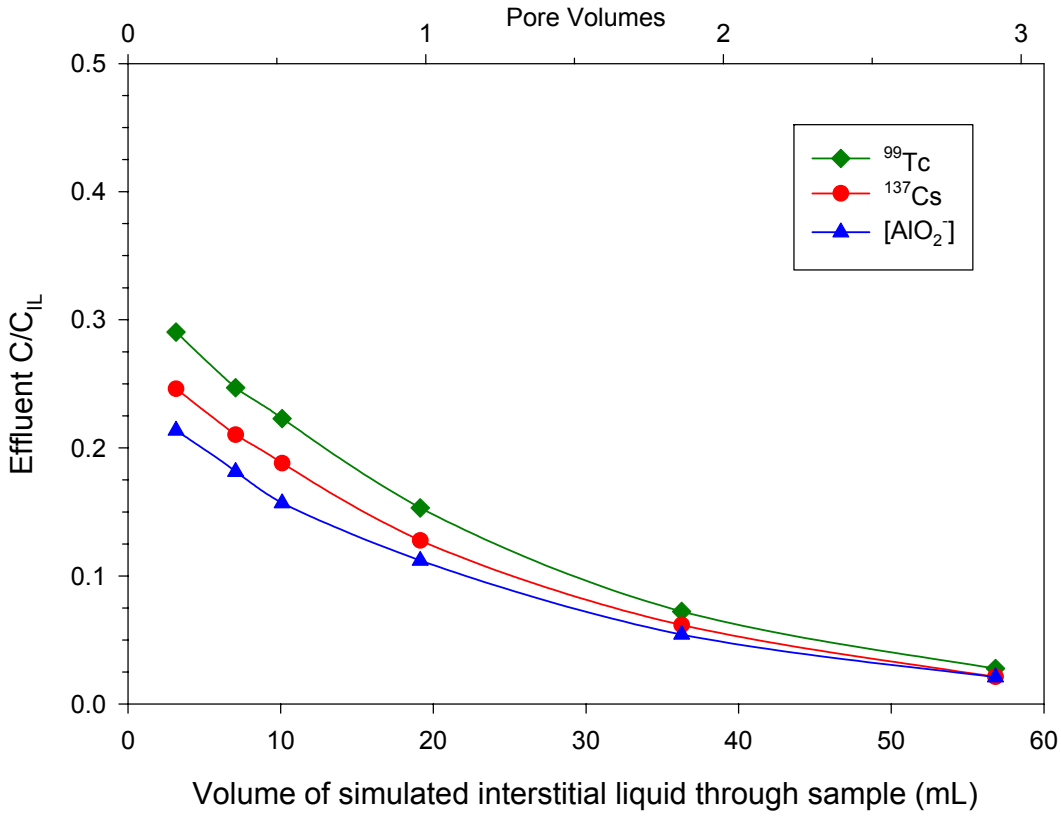

Figure 16: Normalized effluent concentration of ^{137}Cs, ^{99}Tc, and AlO_2^- during falling-head test.

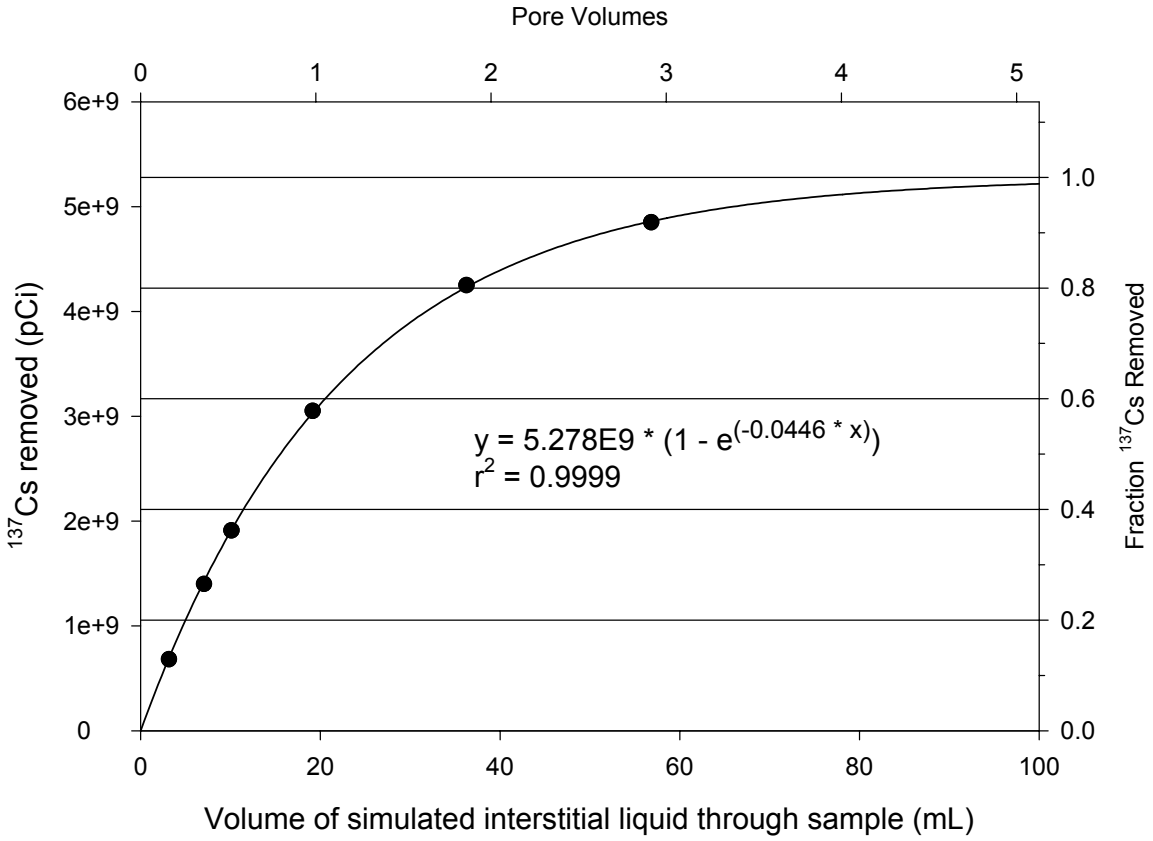

Figure 17: Removal of ^{137}Cs from HTF-609 during permeability testing

Microscopy

Saltcake

Material from each of the three Tank 10H saltcake samples was analyzed by Scanning Electron Microscopy (SEM) and X-ray Diffraction (XRD). Grain size and coherence are among the most notable physical differences within this 36 inch saltcake core. Sample HTF-609, located closer to the top of the 36 inch core is the most "sand-like" with large, loose, distinct grains. In contrast, sample HTF-611 from the bottom of the core is more consolidated with numerous small precipitates covering and perhaps cementing larger grains together. Sample HTF-610, located in the middle of the core, appears to have physical characteristics in between these other two samples. These physical differences will likely influence the amount of macroporosity and microporosity of the salt. Note that some of the solids may have formed after tank sampling due to temperature effects, or during sample preparation due to drying.

Sample HTF-609:

Sample HTF-609 consists of distinct, sand-like grains ranging in size from 50 μm to approximately 1 mm in their longest direction (Figure 18). The grains vary in external morphology. The blocky grains tend to have grain faces similar in size in two or three directions producing the cubic or rectangular shaped grains. Other grains appear to be shorter in length in one direction creating a thinner "platy" shape. Backscattered and elemental spectra of the large blocky grains indicate that they consist primarily of sodium and nitrogen (Figure 19 and Figure 21). These findings are consistent with the results from x-ray diffraction, which show that the mineralogical composition consisted of sodium nitrate (Figure 20).

Closer examination of the blocky grains in this sample reveals the presence of mercury and chromium in localized areas (Spot 7 in Figure 21). Secondary precipitates with zinc and aluminum are also evident (Spot 9 in Figure 21). Examination of the smaller grains shows that some of these grains do not consist of a single dominant crystal but are composed of smaller crystals or particulates (Spots 2 and 3 in Figure 22). These grains could possibly result from mineral growth on existing crystals and particulates or from the cementation of small grains. Relative to the overall sample, these are trace quantities of very small particles adhered to a much larger crystal of sodium nitrate. Spot 2 is an example of mineral precipitation around another grain as evident by the different compositions seen in backscattered image (Figure 22). Elemental analysis shows that the massive precipitate, which appears to surround the edges of a smaller crystal, consists of iron, chromium, silicon and sodium. Elemental analysis also suggests the presence of a sodium bearing mineral other than sodium nitrate or sodium sulfate (possibly sodium carbonate or sodium hydroxide) in the smaller grains (Spot 3).

Sample HTF-610:

In contrast to HTF-609, grains in sample HTF-610 appear to be smaller in size (10 to 100 μm) and distinct crystal faces are more difficult to find (Figure 23). Numerous smaller precipitates with varying morphologies and chemistries are evident and appear to mask the larger grains. X-ray diffraction also indicates a variety of minerals in the sample including sodium bearing nitrate, carbonate and sulfate (Figure 24). Not only was the double-salt burkeite present ($Na_6(SO_4)_2CO_3$), but the double-salt sodium carbonate sulfate was observed as well ($Na_6(CO_3)_2SO_4$).

Figure 25 shows an example of the numerous smaller crystals found in this sample. Spots 10 and 12 likely indicate the presence of a sodium sulfate mineral whereas Spot 9 with only sodium is possibly indicative of a sodium carbonate or sodium hydroxide mineral. Figure 26 illustrates one of the few identifiable large blocky grains in the sample together with small secondary precipitates on the edges and corners. The blocky grain has an elemental chemistry similar to Spot 9 in Figure 25 (sodium) whereas the smaller precipitates are similar to Spot 10 in Figure 25 (sodium and sulfur). In contrast with HTF-609, a distinct nitrogen peak is absent from these spectra. These findings are somewhat consistent with the bulk chemistry analysis of this sample, which found a large amount of sulfate (24 wt %) and carbonate (12 wt %) compared to the other samples, and with the XRD results.

Elemental spectra also indicate the presence of iron, aluminum, calcium, mercury and palladium (Spot 11 in Figure 25 and Spots 1 – 6 in Figure 27). Iron and mercury are typically seen as brighter areas on the backscattered images (e.g. Spots 1, 3, 4 & 6 in Figure 27). In Figure 27, the base grain clearly appears to contain iron; however, it is often difficult to ascertain whether the specs of iron and mercury are separate grains or have been incorporated as part of other crystals (e.g. Spots 3, 4 & 6). The presence of iron and mercury in this sample is consistent with bulk chemistry findings and is more typical of the chemistry found in sludge than in saltcake.

Sample HTF-611:

Through visual observation of this sample, it was characterized as a white and hard-packed powder that was not easily scooped from the sample tube. Out of the three samples, it is the most consolidated and least sand-like in appearance. Distinct grains with recognizable crystal faces or morphologies are difficult to find, particularly at low resolution (Figure 28).

X-ray diffraction analysis indicates that the sample's mineralogy is consistent with sodium bearing nitrate, carbonate and zeolite (Figure 29).

At higher resolution, abundant small precipitates appear to mask larger crystals and possibly cement grains together (Figure 30). Spot 1, a larger crystal in Figure 30,, consists of sodium and nitrogen. Based on XRD, it may represent a sodium nitrate mineral. Spots 2, 4, 5 and 6 show examples of smaller precipitates, which tend to vary in chemistry. Spot 4 looks sub-cubic and contains sodium and nitrogen (similar to spot 1, the larger crystal). Sulfur, which is present at spots 2 and 6, seems to

occur primarily in the very small precipitates and does not seem as pervasive in this sample as in the previous sample (HTF-610). Spot 6 shows aluminum and silicon in addition to the sodium and sulfur, possibly reflecting a zeolite mineral identified by XRD. Iron and chromium were also identified at spot 3; like sulfur, these elements do not appear as prevalent as they are in the previous sample (HTF-610).

Figure 31 provides closer examination of some of the small precipitates. Elemental analysis indicates that part of the larger crystal consists of sodium and nitrogen (spot 7) similar to the larger crystal in the previous figure. The very fine, intergrown precipitates consist of sodium, sulfur, and aluminum (spot 8) similar to spot 2 in the previous figure. Photos C and D of Figure 31 also show the abundant microporosity in the fine-grained matrix of this sample.

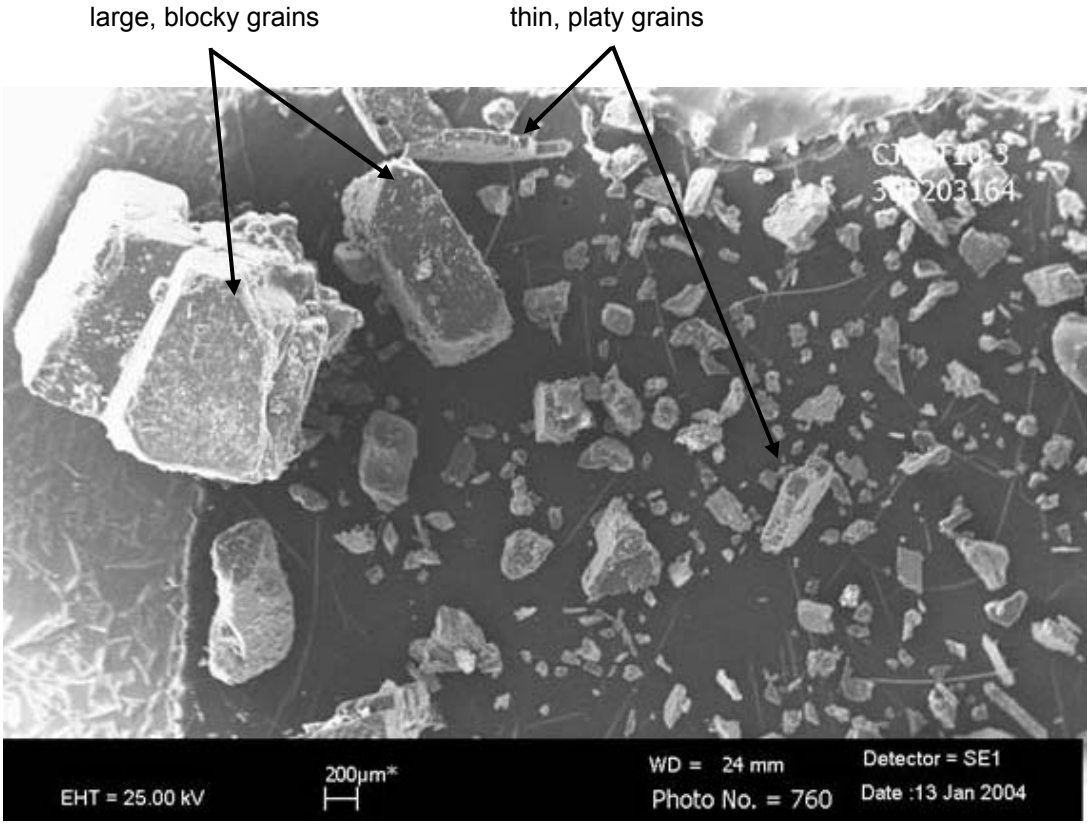

Figure 18: Varying morphology and size of the distinct sand-like grains of sample HTF-609.

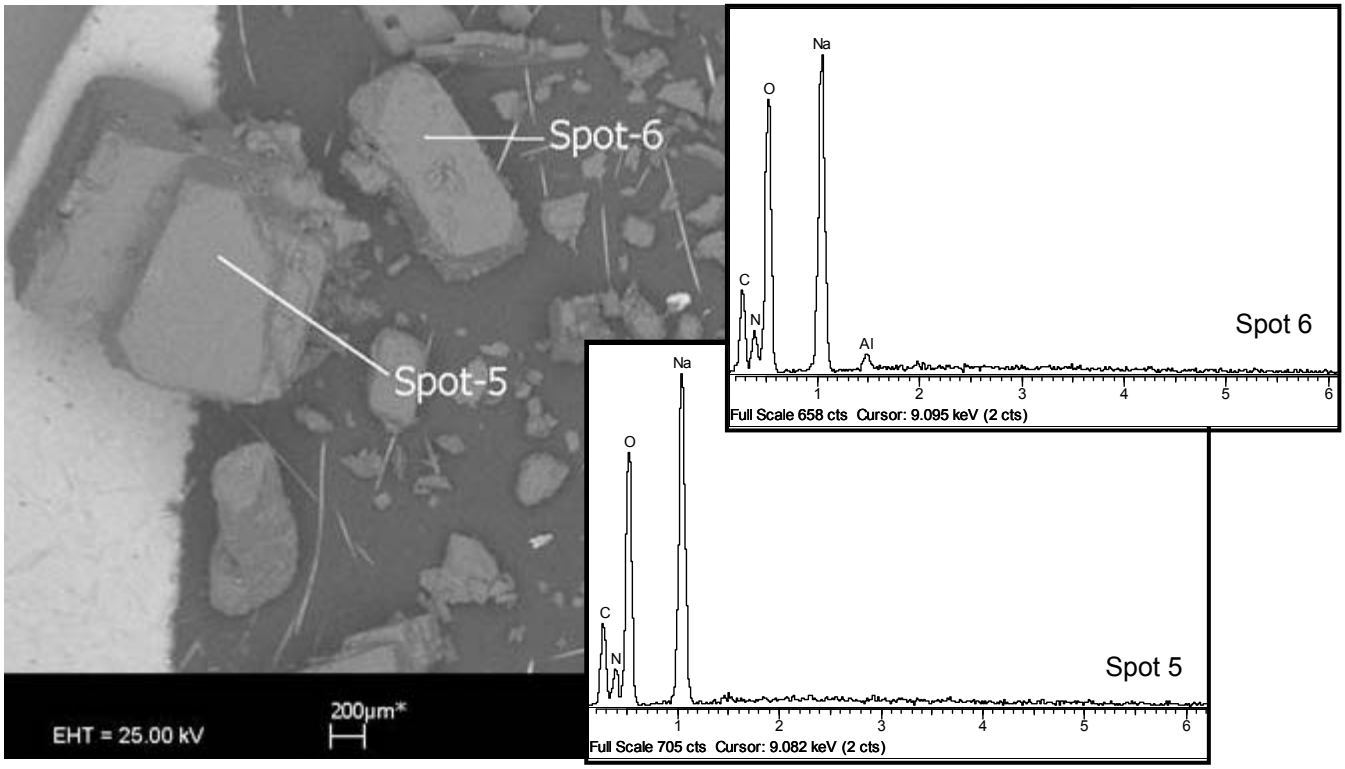

Figure 19: Backscattered image and elemental spectra for large, blocky grains in HTF-609.

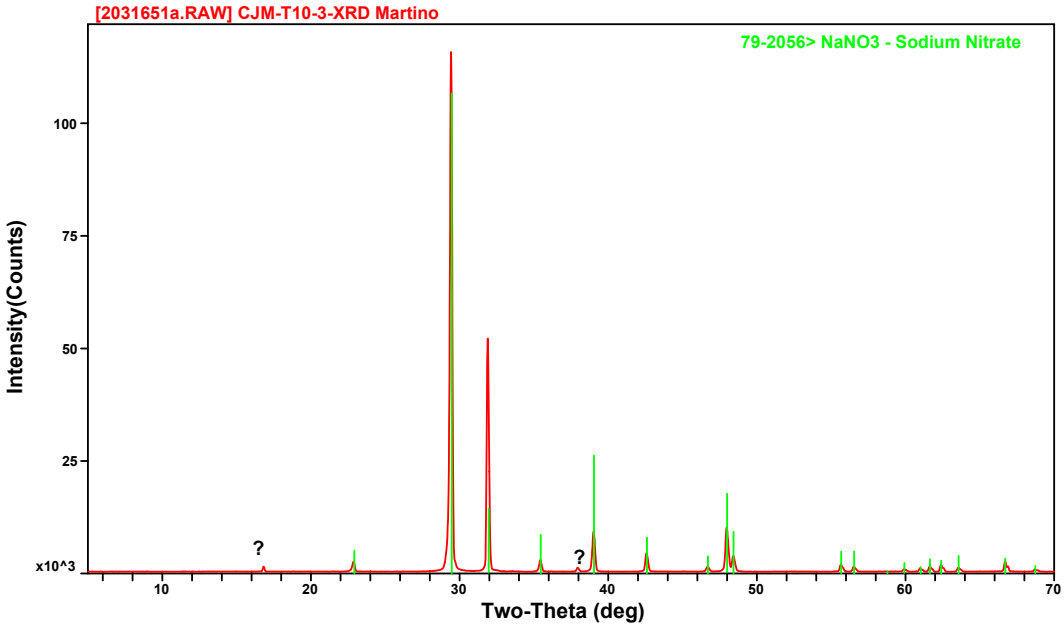

Figure 20: X-ray diffraction analysis of HTF-609

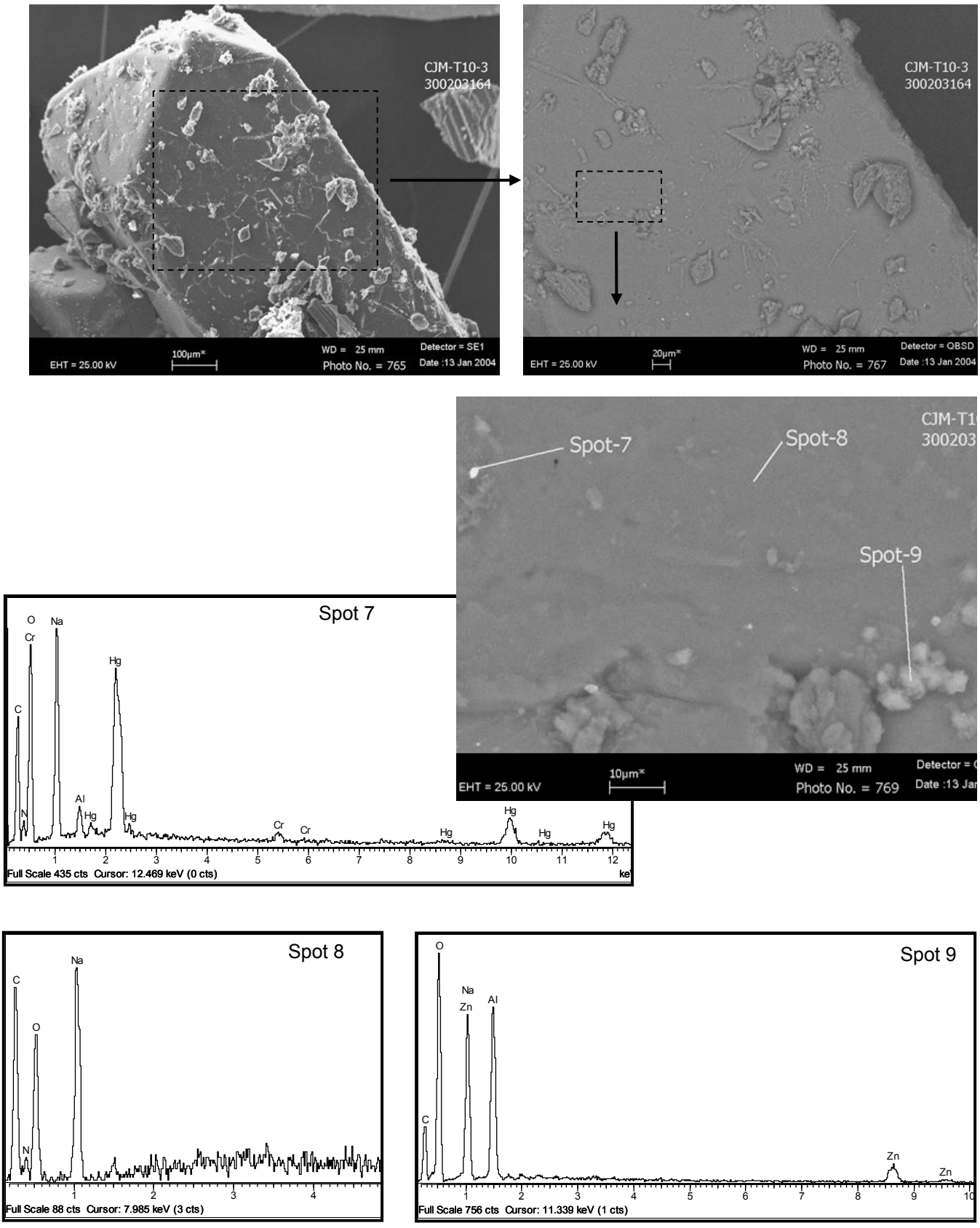

Figure 21: Closer examination of large blocky grains in HTF-609 (secondary electron image on left; backscattered image on right and below with elemental spectra).

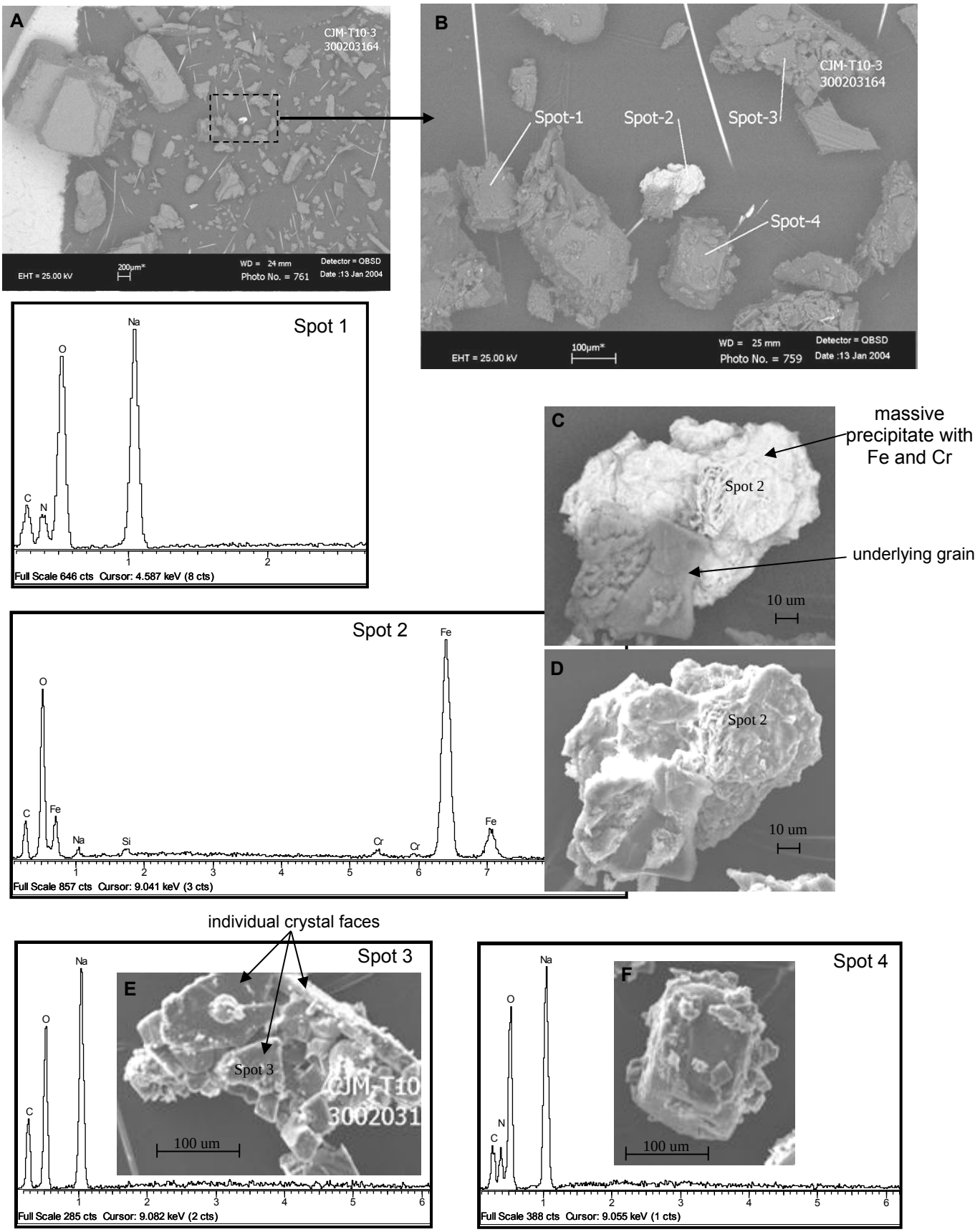

Figure 22: Backscattered (A-C) and secondary electron (D-F) images together with elemental spectra for smaller grains in HTF-609.

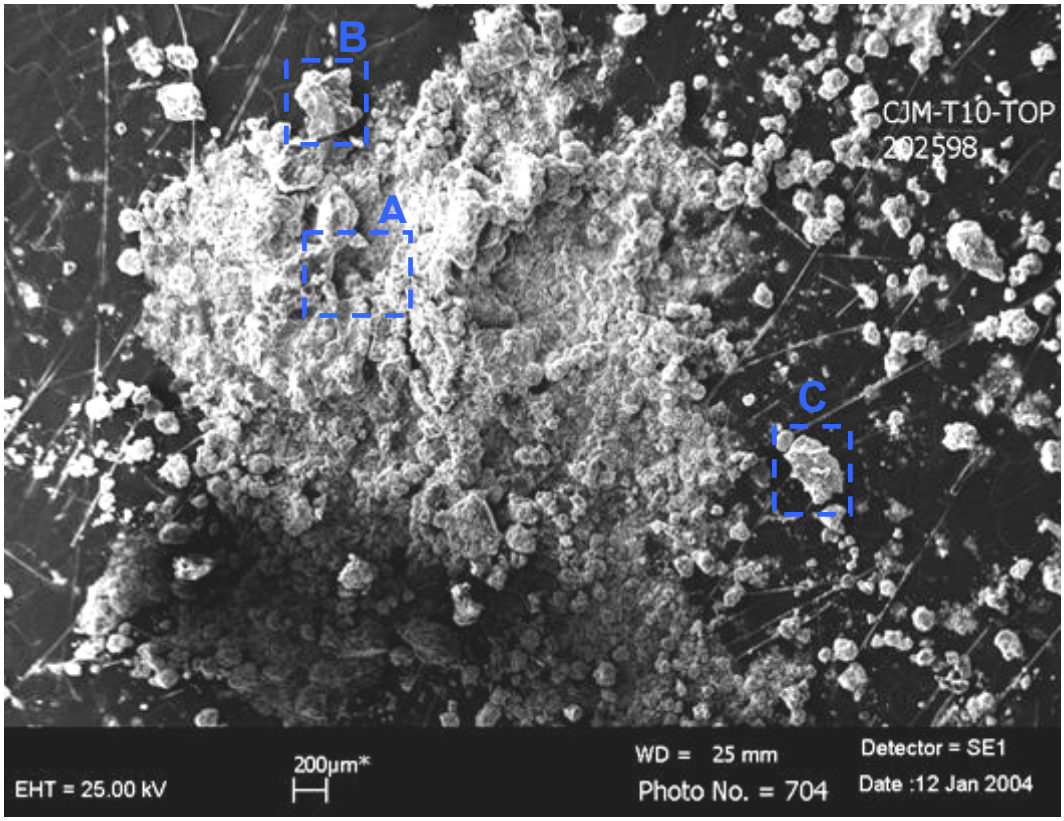

Figure 23: Secondary electron image of grains in sample HTF-610. The highlighted areas (A, B, and C) correspond to Figure 25, Figure 26, and Figure 27, respectively.

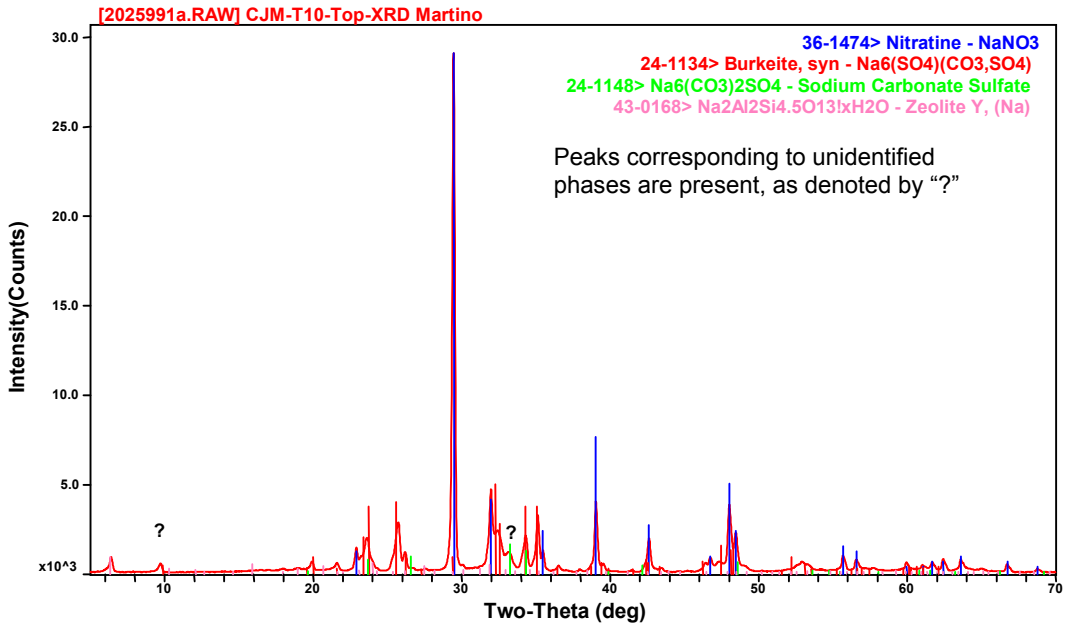

Figure 24: X-ray diffraction analysis for sample HTF-610.

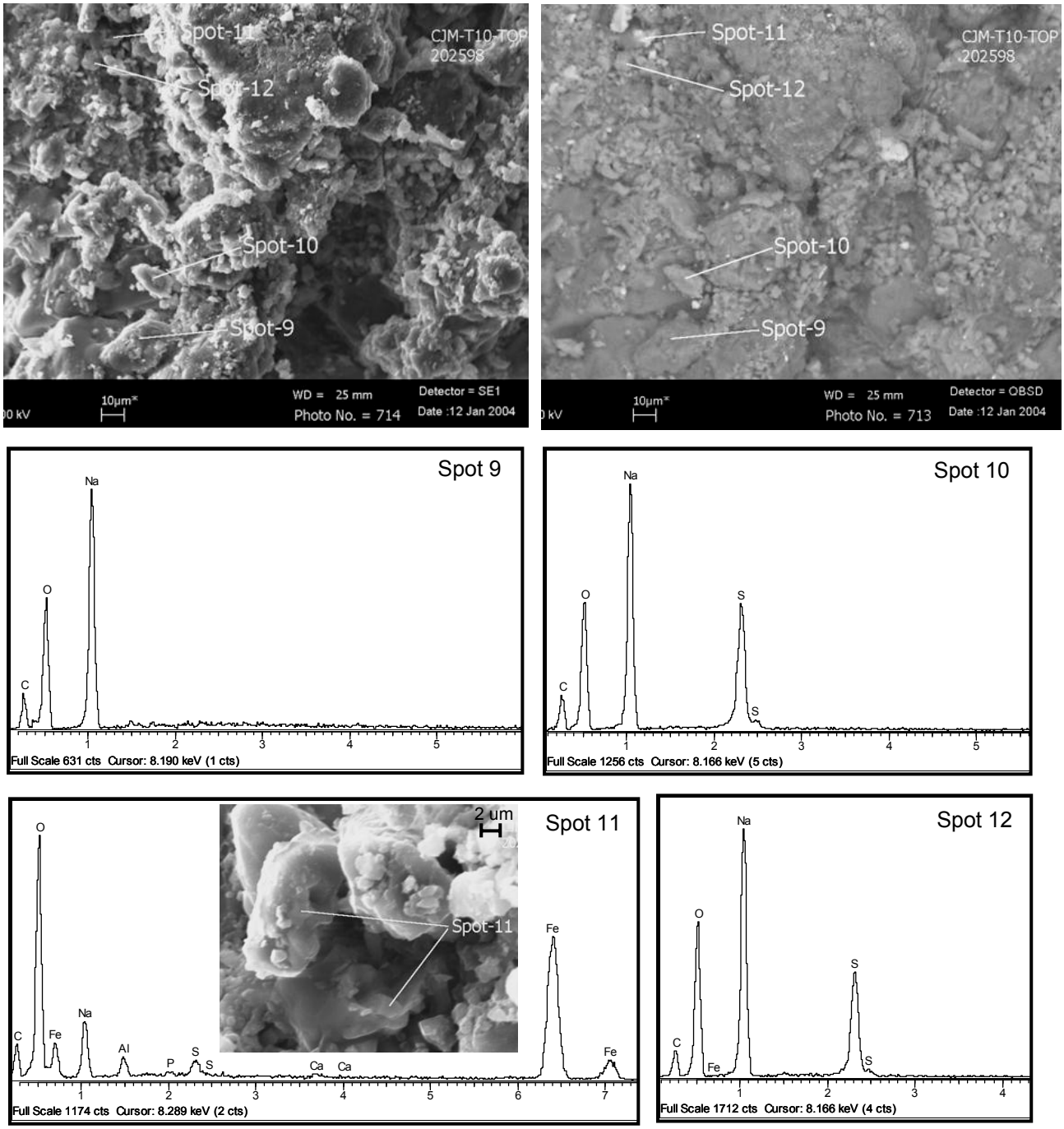

Figure 25: Secondary electron (left and inset) and backscattered (right) images of small grains in HTF-610; location is highlighted as "A" in Figure 23.

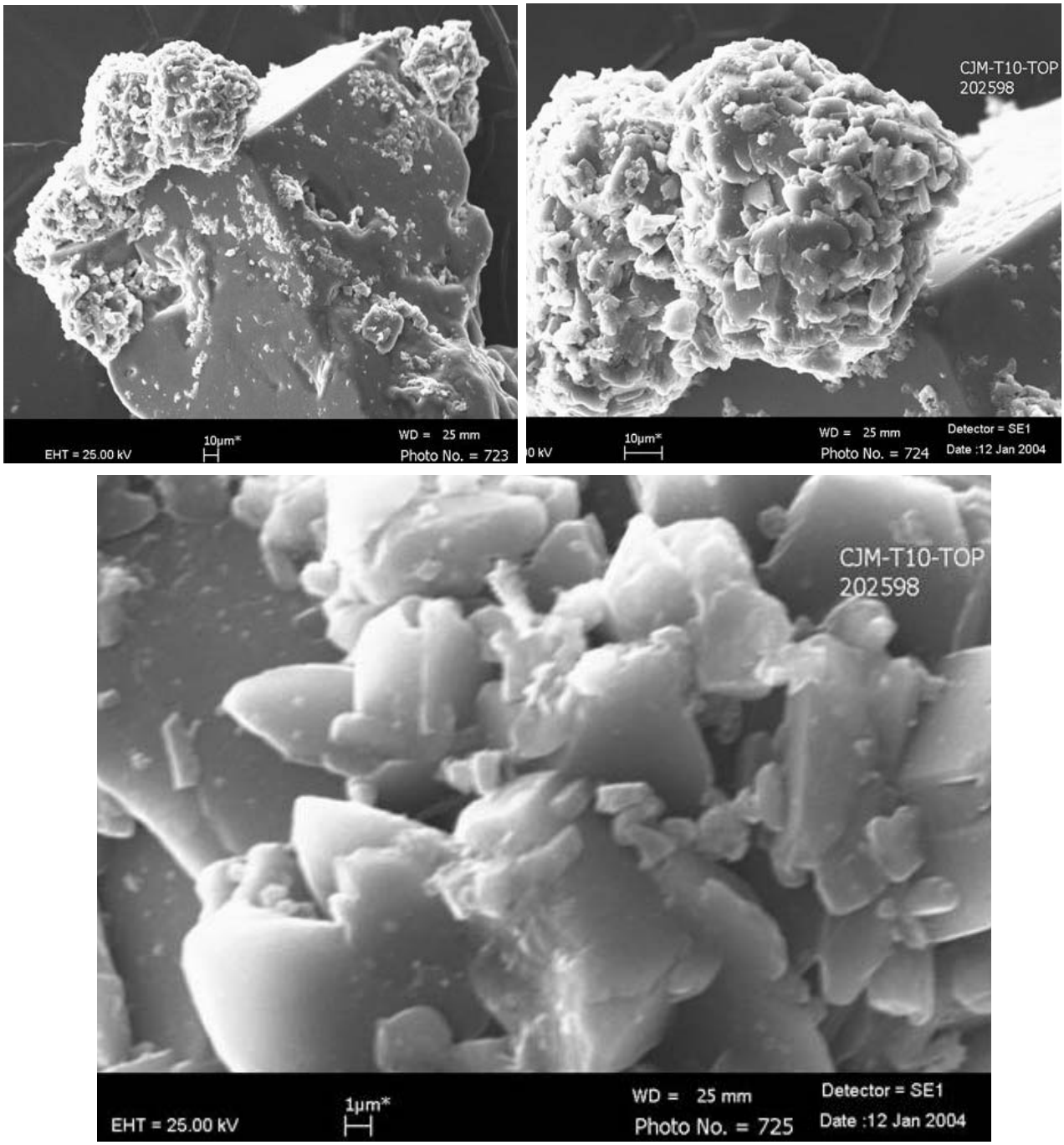

Figure 26: Secondary electron images showing one of the few identifiable blocky grains at low resolution (left) with small, intergrown precipitates (right and bottom); from location "B" in Figure 23 (HTF-610).

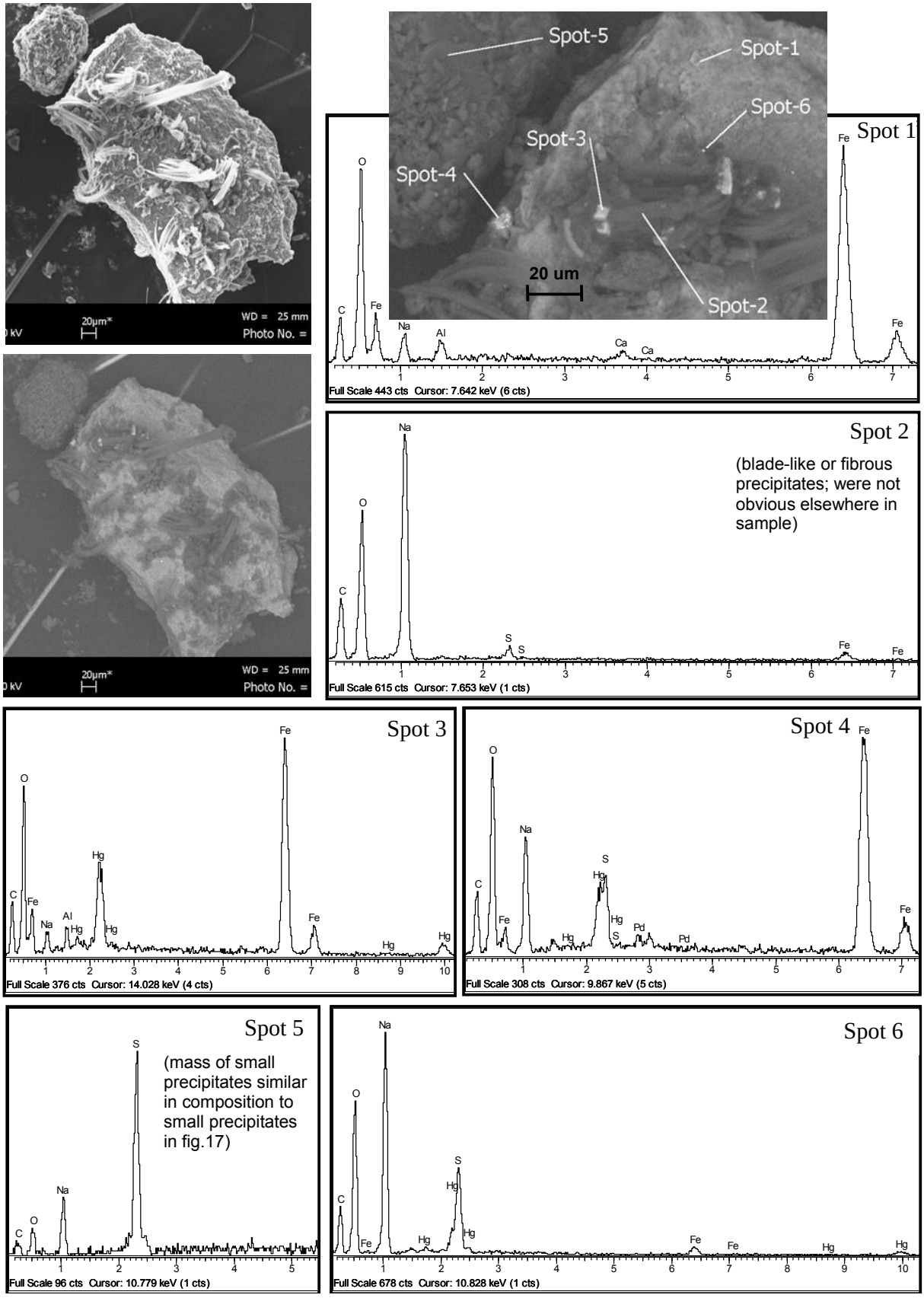

Figure 27: Secondary electron (left) and backscattered (right and inset) images and elemental spectra for grain identified as "C" in Figure 23 (HTF-610).

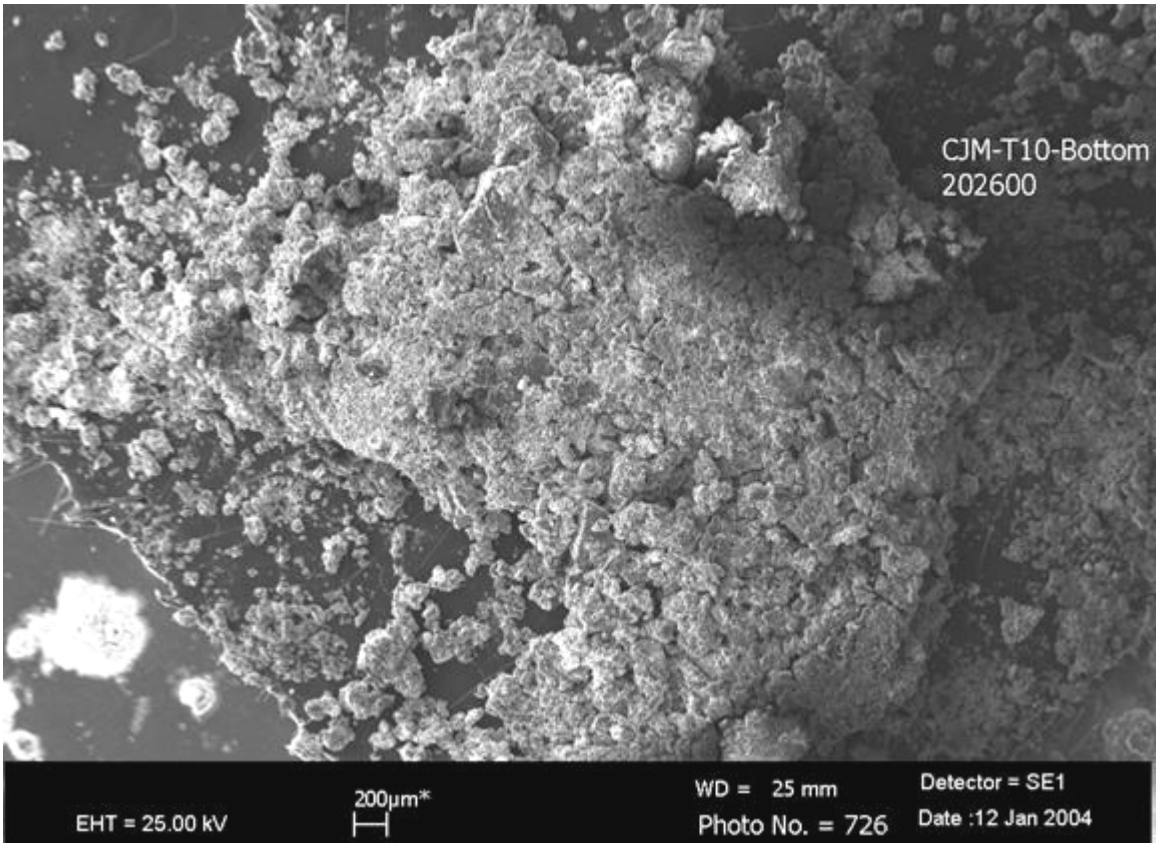

Figure 28: Secondary electron image of grains in sample HTF-611.

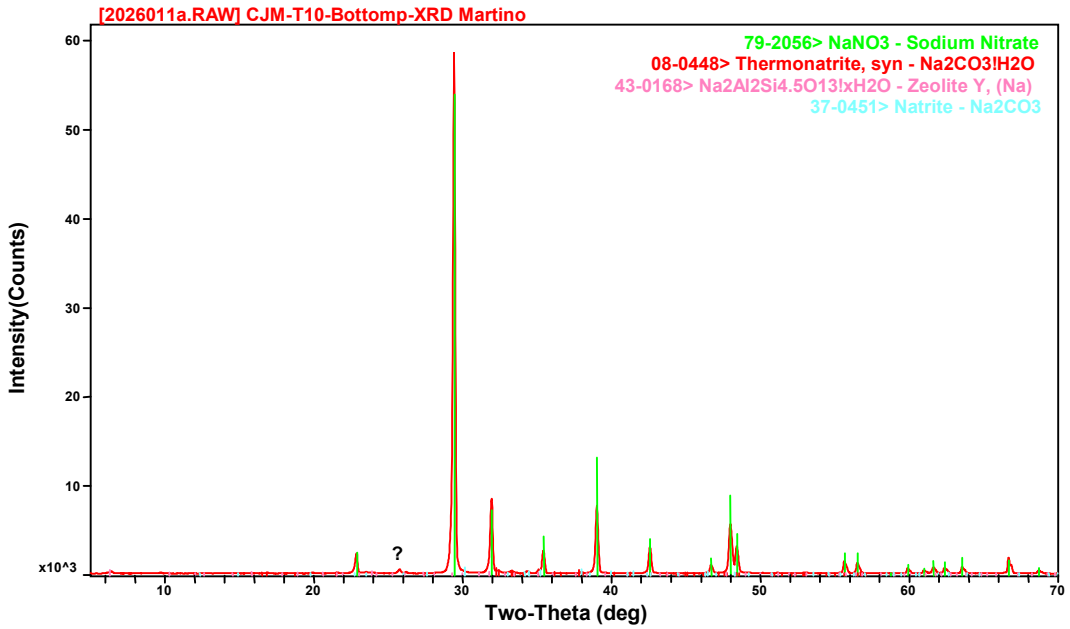

Figure 29: X-ray diffraction analysis for sample HTF-611.

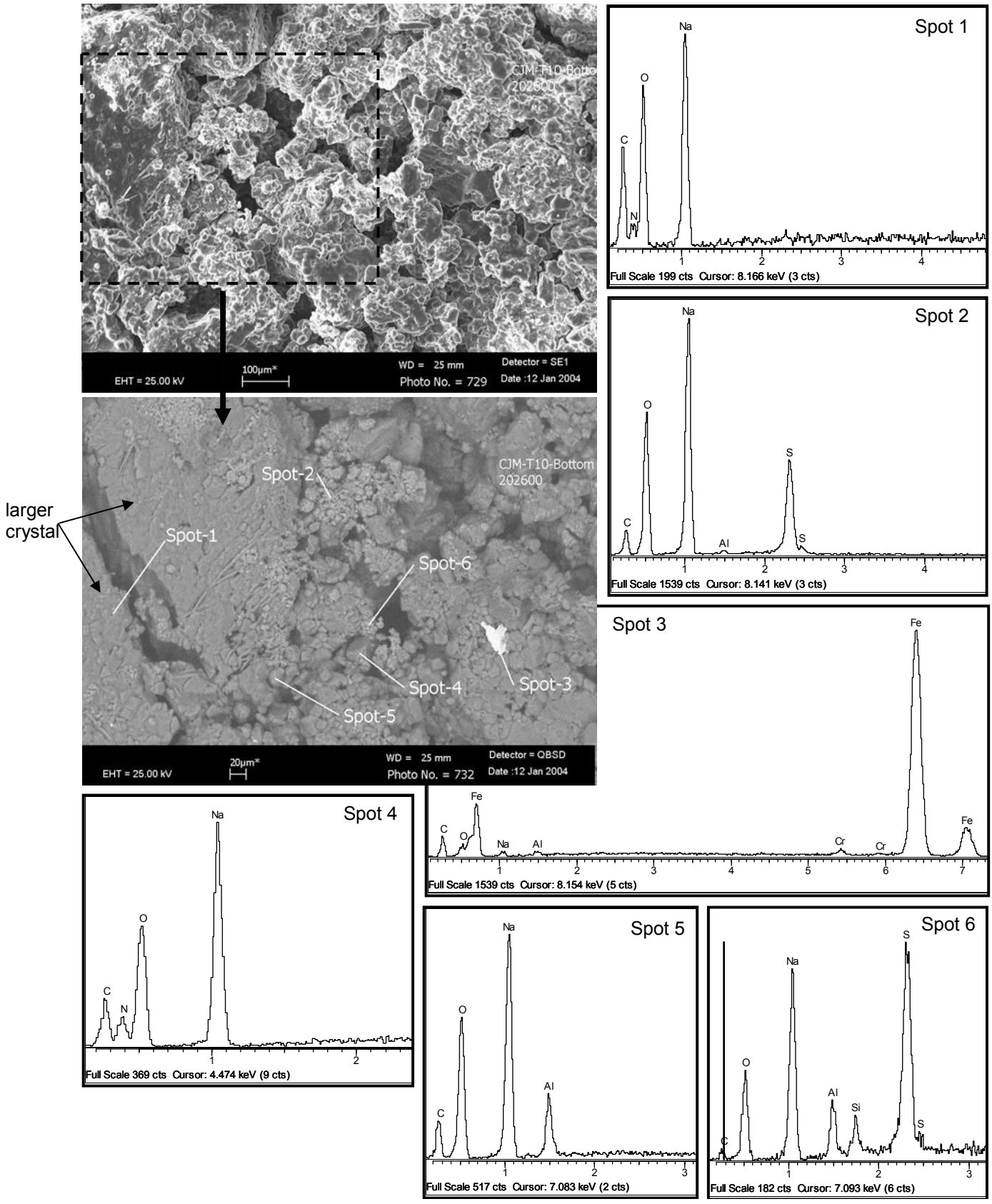

Figure 30: Secondary electron image (top) of small precipitates coating larger grain in HTF-611, with backscattered image (bottom) and elemental spectra for area highlighted in box.

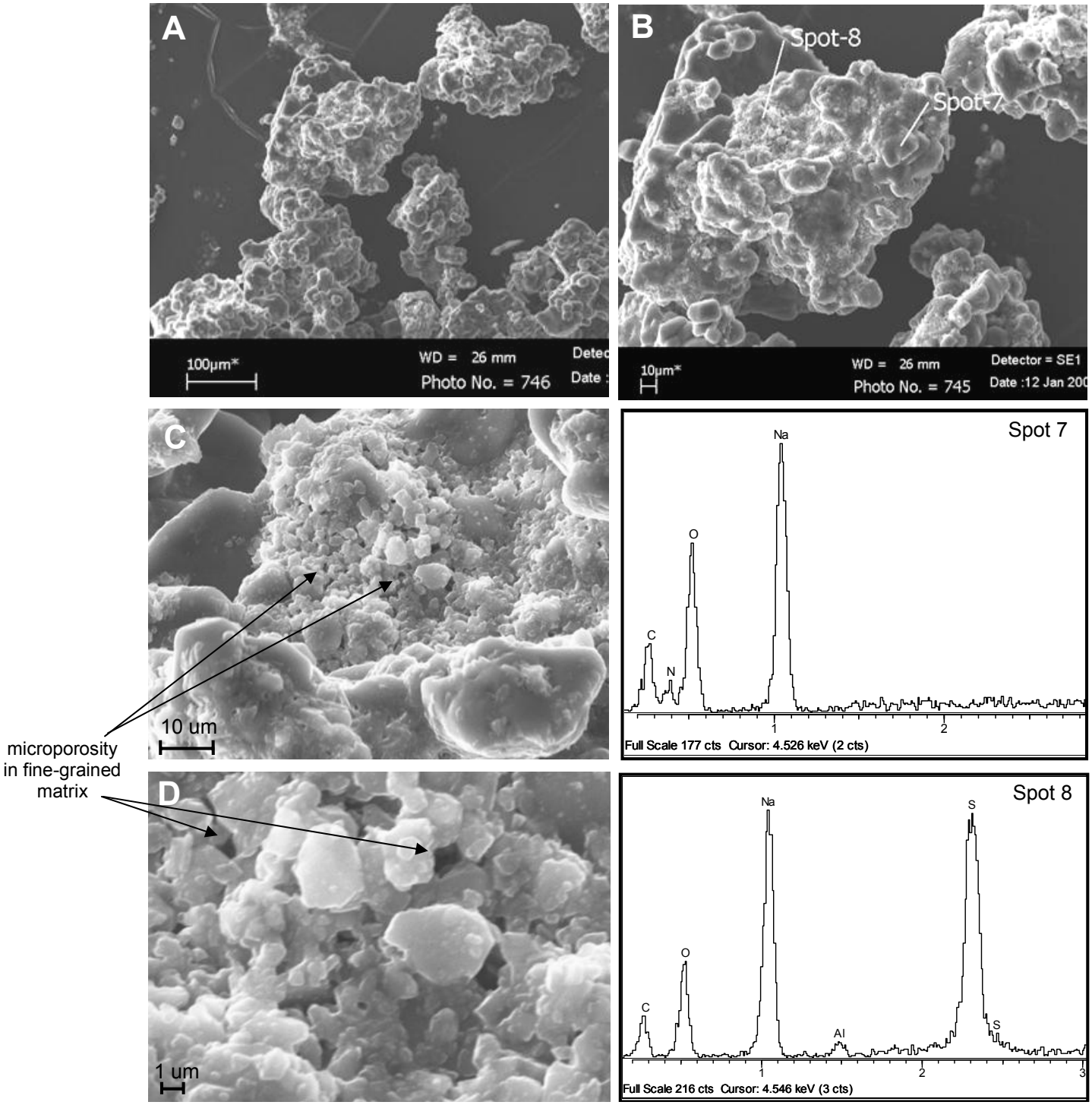

Figure 31: Closer examination of small precipitates in HTF-611; increasing resolution of secondary electron images from A to D.

Residual Insoluble Solids

The filter containing the insoluble solids resulting from the dissolution of drained sample HTF-609 was analyzed by XRD (see Figure 32) and by SEM/EDS. Several crystalline aluminosilicates were identified by XRD, including the sodium aluminosilicate phases cancrinite and sodalite and the calcium aluminosilicate phase stratlingite. A potential Ca-Mn-Mg-Fe-carbonate phase was also noted. The previous Tank 10H salt dissolution was accomplished by the addition of RBOF material from Tank 23H, and previous analyses of Tank 23H suggested that diatomaceous earth and zeolites containing aluminum and calcium were present.[11,12] It is likely that these calcium-containing phases, which are unique to this Tank 10H saltcake sample, were transferred directly from Tank 23H or created during dissolution with RBOF material.

Figure 33, Figure 34, and Figure 35 contain SEM images of the insoluble solids captured on the filter from the draining and dissolution test. The backscatter and EDS analysis revealed that the insoluble solids had a varied makeup, with the abundance of bright areas in the insoluble material corresponding to heavier elements. There was a predominance of mercury throughout the insoluble solids. Sodium, aluminum, and silicon can be seen throughout the solids, confirming that the bulk of the insoluble material is sodium aluminosilicates, like those crystals detected by XRD. Several types of other particles of differing primary composition were observed: one type appeared to be an aluminum oxide or hydroxide (Figure 35) and another type appeared to be an iron oxide or hydroxide (Figure 33, Spot 1). Chromium and iron are also seen throughout the solids. Uranium was detected at different locations in the solids, but did not appear uniform throughout the solids. Traces of other elements, including zinc, calcium, and copper, were noted within the solids.

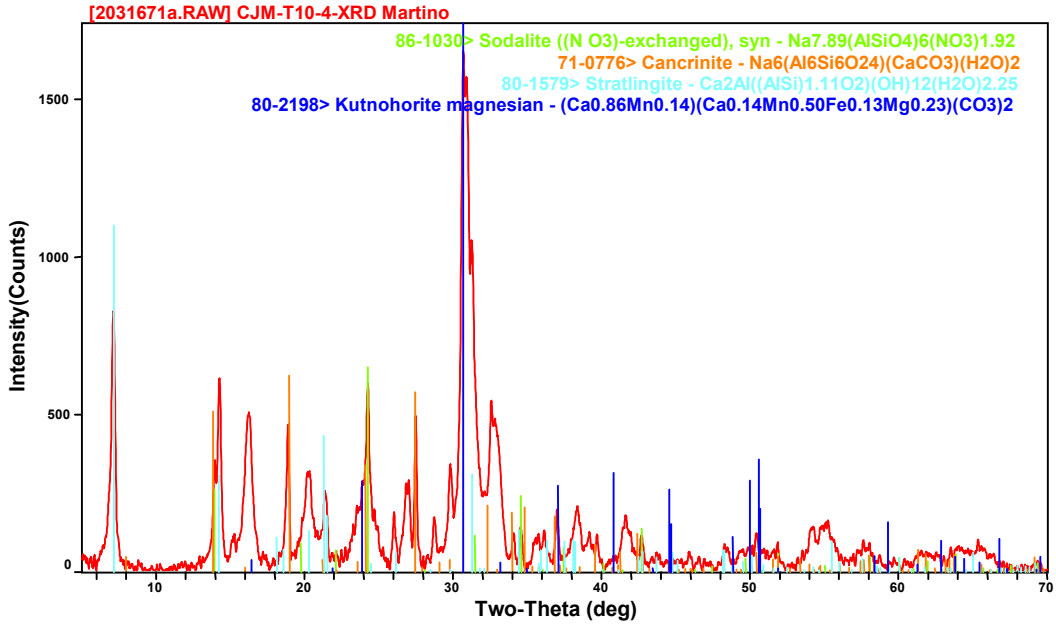

Figure 32: XRD analysis of insoluble solids resulting from dissolution of Tank 10H saltcake

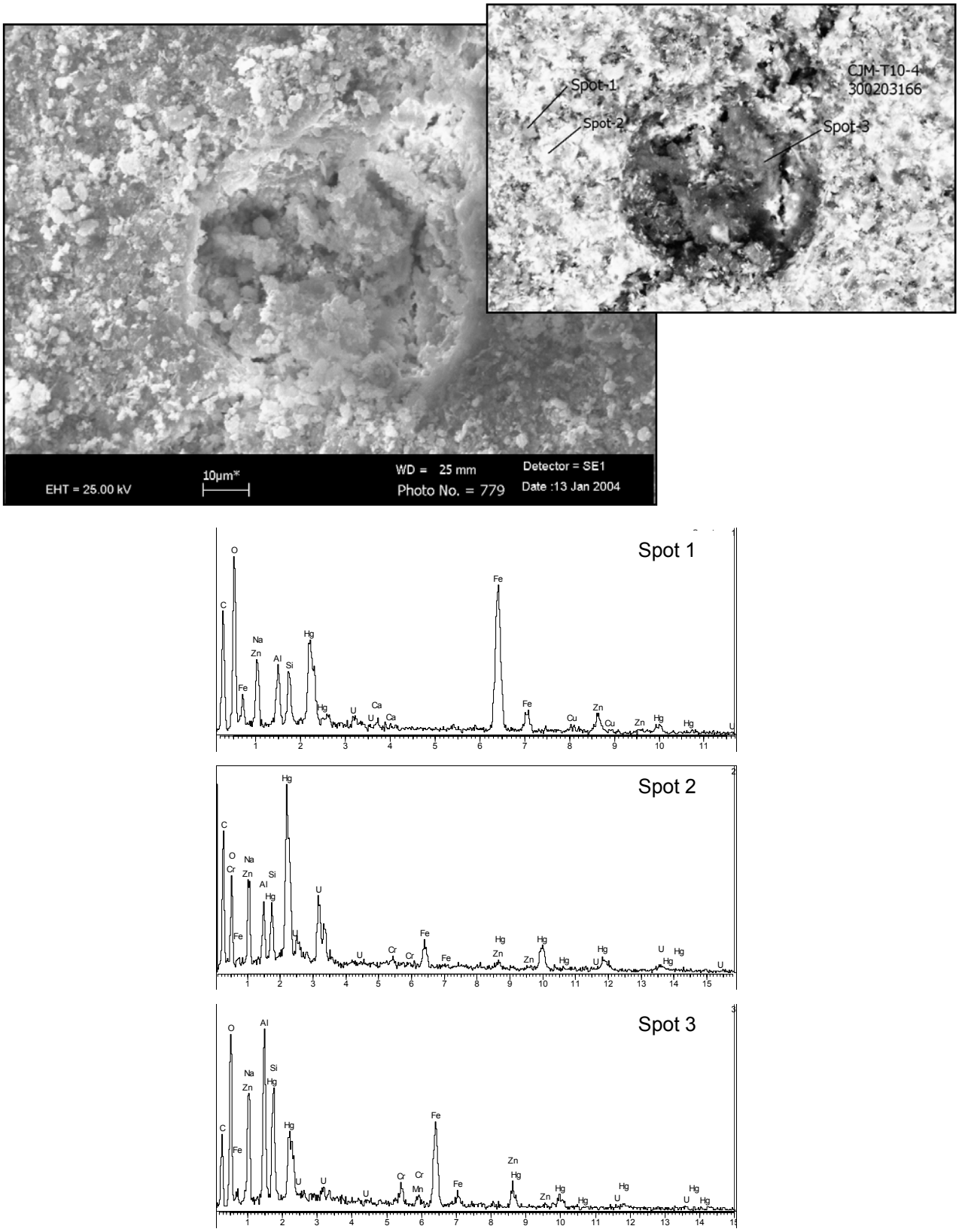

Figure 33: SEM of residual insoluble solids from the draining and dissolution of the bottom of HTF-609, secondary electron (left) and backscattered (right) micrographs, and EDS (below).

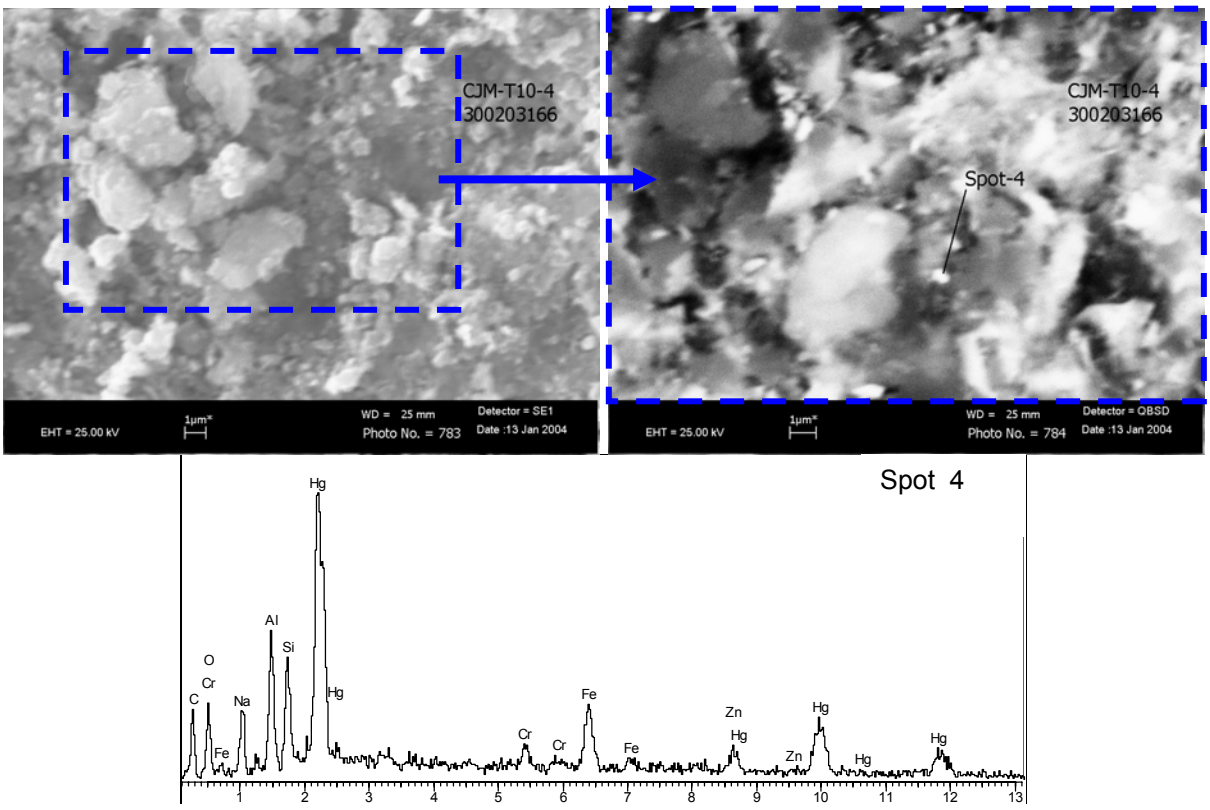

Figure 34: Localized (<0.5 μm) Hg-containing particle(s) in Tank 10H residual insoluble solids.

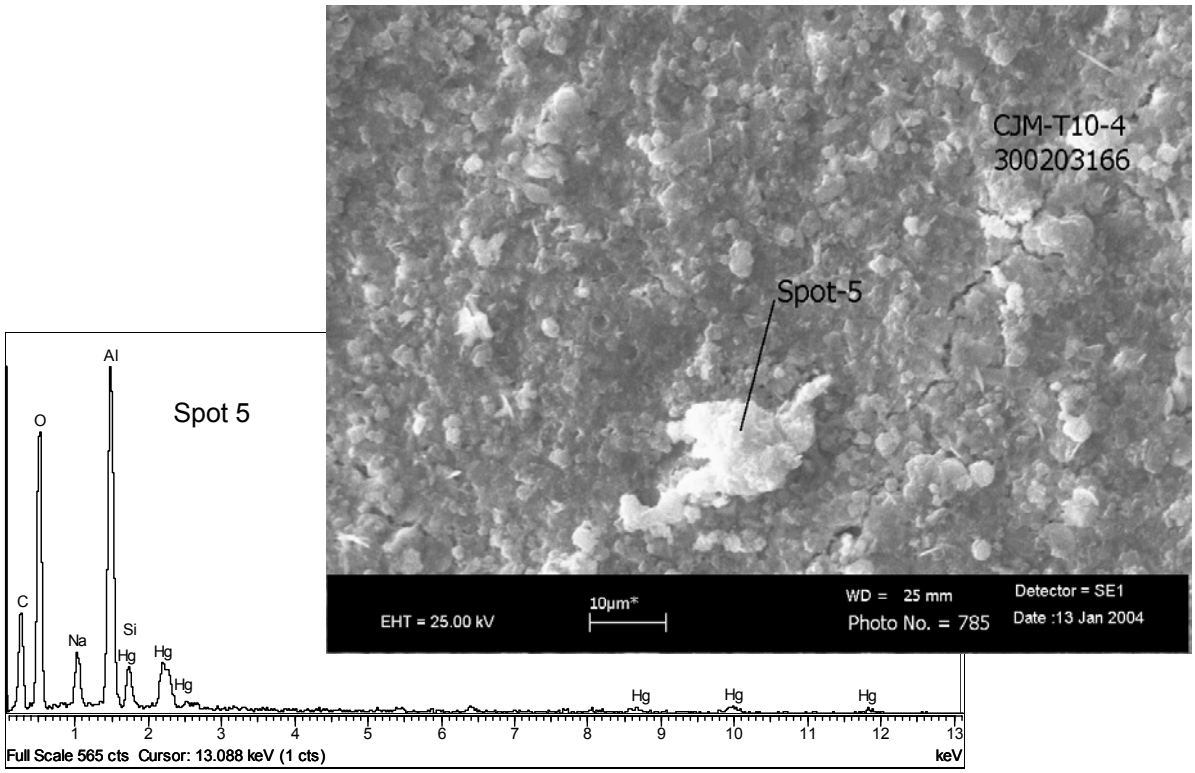

Figure 35: Aluminum hydroxide or oxide in Tank 10H insoluble solids.

Conclusions

This report provides details of the characterization of the Tank 10H saltcake samples (HTF-609, 610, and 611) pulled in October 2003. The three Tank 10H saltcake samples were filled to nearly their capacity, with an average bulk density of 2.06 g/cm^3.

The undrained bulk saltcake from the top of the middle sample (HTF-610) had a water content of 12.8 wt %, a ^{137}Cs activity of 0.94 Ci per gallon of saltcake, an actinide content of 1.3E+6 pCi/g, and a ^{235}U enrichment of 6.6%. The unique characteristic of HTF-610 was the relatively large amount of sulfate (24 wt %) and carbonate (12 wt %), and the relatively small amount of nitrate (24 wt %). The undrained bulk saltcake from the bottom of the bottom sample (HTF-611) had a water content of 4.4 wt %, a ^{137}Cs activity of 0.63 Ci per gallon of saltcake, an actinide content of 1.1E+5 pCi/g, and a ^{235}U enrichment of 23%. HTF-611 had a more typical level of nitrate (64 wt %).

Interstitial liquid drained from the top sample (HTF-609) had a density of 1.43 g/cm^3, a soluble solids content of 47.0 wt %, a ^{137}Cs activity of 3.3 Ci per gallon of interstitial liquid, and an actinide content of 2.6E+4 pCi/mL. Similar results were obtained for interstitial liquid drained from HTF-610.

A flow-through dissolution test was performed on the drained saltcake sample from the bottom of HTF-609. The ^{137}Cs concentration was highest in the effluent from the earliest stages of dissolution and decreased during subsequent stages of the dissolution test, with the bulk dissolved salt effluent having a ^{137}Cs of 0.10 Ci/gal at 4.3 M [Na^+] (corresponding to 0.14 Ci/gal at 6 M [Na^+]).

The average hydraulic conductivity of the top portion of sample HTF-609 was 4.2 * 10^{-4} cm/sec, which is similar to that for a fine to medium grained sand. An estimated 91% of the residual ^{137}Cs in the drained salt sample HTF-609 was displaced by 2.9 pore volumes of simulated interstitial liquid during the falling head permeability test.

Material from each of the three Tank 10H saltcake samples was analyzed by SEM and XRD. Grain size and coherence are among the most notable physical differences within this 36 inch saltcake core, likely influencing the amount of macroporosity and microporosity. The material from the top of HTF-609, the top of the core sample, has large, loose, distinct grains. In contrast, sample HTF-611, from the bottom of the core, is more consolidated with numerous small precipitates covering and perhaps cementing larger grains together. Residual insoluble solids from the drained and dissolved Tank 10H sample HTF-609 contained sodium aluminosilicates, calcium aluminosilicates, mercury, iron, chrome, uranium, and a variety of other components.

Quality Assurance

This work satisfies the requirements of the original task technical and quality assurance plan.[13] Laboratory Notebooks WSRC-NB-2003-00072, WSRC-NB-2003-00233, and various ADS notebooks contain the experimental data.

Acknowledgements

The authors thank the following for their important contributions to this project: John Sessions, Glen Johnson, and Dennis Conrad of the Closure Business Unit; Nancy Gregory and Sharon Smith in SRTC Waste Processing Technology; Monica Jenkins, Mona Galloway, Carolyn Conley, Ron Blessing and many others in SRTC Shielded Cells Operations; Tom Nance and Dan Krementz of SRTC Remote Specialty Equipment; Curt Sexton of the SRTC Glass-blowing Shop; Miles Denham of SRTC Environmental Restoration Technology; and Leigh Brown, Dave Diprete, Ceci Diprete, Theresa Eddy, June Hart, Damon Click, Bill Boyce, Mira Malek, Chuck Coleman, Beverly Burch, John Young,

Amy Ekechukwu, Robert Ray, Michael Whitaker, Art Jurgensen, Dave Missimer, Mike Summer, Wilson Smith, Marti Finney, and many technicians of SRTC Analytical Development.

References

[1] J. R. Sessions, "Saltcake Characterization to Support Closure Activities," CBU-SPT-2003-00126, Rev. 0, July 17, 2003.

[2] D. T. Conrad, "LCS Sampling and Analysis Plan for Process Validation," CBU-SPT-2003-00164, Rev. 0, September 9, 2003.

[3] J. A. Pike, "Tank 41 Salt Dissolution Flowsheet Modeling," WSRC-TR-2002-00209, Rev. 0, May 1, 2002.

[4] G. L. Albert and J. C. Bailey, "Tank 10 Salt Removal Demonstration Details," DPSP 79-17-11, April 11, 1979.

[5] R. L. Nichols and C. J. Martino, "Hydraulic Properties of Saltcake Samples from Tank 41H (U)" WSRC-TR-2003-00543, Rev. 0, January 2004.

[6] C. J. Martino, R. L. Nichols, D. J. McCabe, M. R. Millings, and M. E. Denham, "Tanks 3F and 2F Saltcake Core and Supernate Sample Analysis," WSRC-TR-2004-00131, Revision 0, March 26, 2004.

[7] C. J. Martino and M. R. Poirier, "Tank 31H Saltcake Dissolution Tests," WSRC-TR-2002-00388, Rev. 0, February 27, 2003.

[8] G. P. Flach, "Porous Medium Analysis of Interstitial Liquid Removal from Tank 41 and Tank 3 (U)," WSRC-TR-2003-00533, Rev. 0, February 2004.

[9] K. Staheli and J. F. Peters, "Interstitial Fluid Displacement for Preferential Recovery of Cesium from Saltcake," U.S. Army Corps of Engineers Technical Report GL-98-3, April 1998.

[10] J. N. Brooke, J. F. Peters, and K, Staheli, "Hydrological Methods Can Separate Cesium from Nuclear Waste Salt Cake," WSRC-TR-99-00358, October 1999.

[11] J. R. Fowler, "Analysis of tank 23H Sludge," DPST-84-342, February 28, 1984.

[12] D. T. Hobbs, "Analysis of Tank 23 Sludge Sample," DPST-84-972, December 28, 1984.

[13] R. L. Nichols and C. J. Martino, "Task Technical and Quality Assurance Plan for the Characterization of Drained Low-Curie Saltcake," WSRC-RP-2003-00319, Rev. 1, June 3, 2003.

Appendix

Table 11: Undrained Bulk Saltcake rad. chem. results (pCi/g)

Tank 10H	HTF-610		HTF-611	
(pCi/g)	Average	St. Dev.	Average	St. Dev.
^{14}C	2.2E+04	--	--	
^{90}Sr	5.36E+07	6.4E+06	1.43E+06	1.2E+05
^{137}Cs	1.14E+08	9E+06	8.36E+07	3.4E+06
^{238}Pu	1.27E+06	1.6E+05	9.86E+04	7.1E+03
$^{239/240}Pu$	1.77E+04	1.6E+03	5.4E+03	4.9E+03
^{241}Am	2.35E+04	1.18E+04	1.44E+03	4.1E+02

Table 12: Undrained Bulk Saltcake AA results (g/100g)

Tank 10H	HTF-610		HTF-611	
(g/100g)	Average	St. Dev.	Average	St. Dev.
As	*< 2.66E-04*	--	*< 2.68E-04*	--
K	1.98E-02	1.9E-03	1.43E-02	3E-04
Se	3.51E-04	4.3E-05	*< 2.68E-04*	--
Hg	5.03E-02	4E-04	4.07E-03	7E-05

Table 13: Undrained Bulk Saltcake IC, wet chemistry, and TIC/TOC results (g/100g)

Tank 10H	HTF-610		HTF-611	
(g/100g)	Average	St. Dev.	Average	St. Dev.
NO_3^-	2.38E+01	2.2E+00	6.40E+01	1.8E+00
NO_2^-	9.43E-01	2.83E-01	9.13E-01	2.47E-01
SO_4^{2-}	2.35E+01	3.6E+00	2.36E+00	6.2E-01
PO_4^{3-}	*< 5.01E-01*	--	*< 4.89E-01*	--
Cl^-	*< 1.00E-01*	--	*< 9.77E-02*	--
F^-	*< 1.00E-01*	--	*< 9.77E-02*	--
$C_2O_4^{2-}$	1.42E-01	3.6E-02	3.66E-01	7.3E-02
CHO_2^-	*< 5.01E-01*	--	*< 4.89E-01*	--
Free OH^-	7.30E-01	1.89E-01	4.94E-01	4.9E-02
CO_3^{2-} (TIC) [a]	1.17E+01	6E-01	1.46E+00	8E-03
TOC [a]	4.5E-01	5E-02	1.9E-01	2E-02

Note a: due to inconsistencies with data not included in this memo, the TIC/TOC for HTF-610 will be reanalyzed.

Table 14: Undrained Bulk Saltcake ICP-ES results (g/100g)

Tank 10H	HTF-610		HTF-611	
(g/100g)	Average	St. Dev.	Average	St. Dev.
Ag	1.43E-03	2.7E-04	*< 8.04E-04*	--
Al	2.86E-01	3.0E-02	2.04E-01	5E-03
B	*< 8.63E-02*	--	*< 8.68E-02*	--
Ba	1.23E-03	3.1E-04	*< 8.04E-04*	--
Ca	</=2.65E-02	3.4E-03	*< 2.43E-02*	--
Cd	*< 1.06E-03*	--	*< 1.07E-03*	--
Ce	*< 1.32E-02*	--	*< 1.33E-02*	--
Cr	9.44E-03	7.43E-03	1.15E-03	1.4E-04
Cu	</=1.85E-03	2.8E-04	*< 1.66E-03*	--
Fe	8.99E-01	3.12E-01	1.53E-02	3.9E-03
Gd	*< 1.44E-03*	--	*< 1.45E-03*	--
K	*< 5.07E-01*	--	*< 5.10E-01*	--
La	*< 1.06E-03*	--	*< 1.07E-03*	--
Li	*< 4.53E-03*	--	*< 4.55E-03*	--
Mg	*< 3.30E-03*	--	*< 3.32E-03*	--
Mn	2.88E-02	5.7E-03	*< 1.18E-03*	--
Mo	*< 1.09E-02*	--	*< 1.09E-02*	--
Na	2.84E+01	2.0E+00	2.58E+01	4E-01
Ni	</=6.07E-03	3.30E-03	*< 4.02E-03*	--
P	</=3.11E-02	6.3E-03	*< 2.60E-02*	--
Pb	*< 1.31E-02*	--	*< 1.32E-02*	--
S	7.84E+00	8.1E-01	6.88E-01	2.5E-02
Sb	*< 8.04E-03*	--	*< 8.09E-03*	--
Si	4.43E-02	1.15E-02	6.70E-03	5.9E-04
Sn	</=1.38E-02	1.3E-03	*< 1.31E-02*	--
Sr	</=5.79E-03	6.9E-04	*< 5.36E-03*	--
Ti	7.98E-04	2.53E-04	3.21E-04	2.1E-05
V	*< 5.86E-04*	--	*< 5.89E-04*	--
Zn	1.53E-02	1.4E-03	4.09E-03	2.2E-04
Zr	</=6.54E-04	8.1E-05	*< 6.43E-04*	--

Table 15: Undrained Bulk Saltcake ICP-MS results (g/100g)

Tank 10H	HTF-610		HTF-611	
(g/100g)	Average	St. Dev.	Average	St. Dev.
Mass 59	9.0E-05	6.1E-05	*< 1.4E-05*	--
Mass 88	1.7E-04	4E-05	*< 1.7E-05*	--
Mass 99	2.91E-04	1.7E-05	1.26E-04	3E-06
Mass 101	3.48E-04	6.3E-05	1.07E-04	7E-06
Mass 133	3.12E-04	2.6E-05	2.09E-04	4E-06
Mass 135	4.74E-05	5.0E-06	2.87E-05	1.5E-06
Mass 137	1.06E-03	1.3E-04	1.39E-04	6E-06
Mass 138	2.12E-04	5.6E-05	</=4.2E-06	1.8E-06
Mass 230 – 231	*< 1.5E-05*	--	*< 1.5E-05*	--
Mass 232	1.91E-03	2.7E-04	*< 1.5E-05*	--
Mass 233	9.4E-05	1.8E-05	3.9E-05	6E-06
Mass 234	3.1E-05	3E-06	1.9E-05	4E-06
Mass 235	6.23E-04	8.5E-05	5.16E-04	5E-06
Mass 236	1.91E-04	2.5E-05	1.43E-04	8E-06
Mass 237	7.4E-05	2.9E-05	2.3E-05	7E-06
Mass 238	8.46E-03	1.19E-03	1.53E-03	1.4E-04
Mass 239	2.1E-05	9E-07	*< 1.5E-05*	--
Mass 240 – 244	*< 1.5E-05*	--	*< 1.5E-05*	--

Table 16: Undrained Bulk Saltcake ^{235}U Enrichment

Tank 10H	HTF-610		HTF-611	
	Average	St. Dev.	Average	St. Dev.
Total U (g/100g)	9.40E-03	1.32E-03	2.25E-03	1.5E-04
^{235}U / Total U (wt. fraction)	0.0663	0.0003	0.230	0.014

Table 17: Drained Interstitial Liquid rad. chem. results (pCi/mL)

Tank 10H	HTF-609 IL		HTF-610 IL
(pCi/mL)	Average	St. Dev.	
^{90}Sr	2.40E+04	1.8E+03	--
^{137}Cs	8.79E+08	1.1E+07	9.78E+08
^{238}Pu	2.35E+04	1E+02	1.48E+04
$^{239/240}Pu$ [a]	2.63E+03	5.4E+02	3.55E+03
^{241}Am	*< 1.42E+03*	--	*< 1.10E+03*

Note a: $^{239/240}Pu$ is likely biased high due to the low levels in the sample approaching the level in the blank.

Table 18: Drained Interstitial Liquid IC, wet chemistry, and TIC/TOC results (mg/L)

Tank 10H	HTF-609 IL		HTF-610 IL
(mg/L)	Average	St. Dev.	
NO_3^-	2.10E+05	1.2E+04	2.03E+05
NO_2^-	6.82E+04	4.5E+03	1.11E+05
SO_4^{2-}	5.42E+03	0E+00	3.82E+03
PO_4^{3-}	2.01E+03	7E+01	2.05E+03
Cl^-	</=1.87E+02	0E+00	*< 9.31E+01*
F^-	*< 1.87E+02*	--	*< 9.31E+01*
$C_2O_4^{2-}$	*< 9.35E+02*	--	*< 4.66E+02*
CHO_2^-	*< 9.35E+02*	--	*< 4.66E+02*
Tot. Base (M)	3.78E+00	2.4E-01	5.21E+00
Free OH^-	6.03E+04	2.84E+04	4.96E+04
CO_3^{2-} (TIC)	2.16E+04	4.5E+03	8.23E+03
TOC	1.9E+03	5E+02	4.03E+03
OH^- (calculated)	5.19E+04	--	7.23E+04

Table 19: Drained Interstitial Liquid ICP-ES results (mg/L)

Tank 10H	HTF-609 IL		HTF-610 IL
(mg/L)	Average	St. Dev.	
Ag	*< 1.41E+01*	--	*< 3.85E+00*
Al	1.88E+04	8E+01	2.42E+04
B	*< 1.52E+03*	--	*< 6.37E+01*
Ba	*< 1.41E+01*	--	6.00E+00
Ca	*< 4.25E+02*	--	1.24E+01
Cd	*< 1.88E+01*	--	*< 1.16E+01*
Ce	*< 2.32E+02*	--	6.63E+01
Cr	1.21E+02	2E+00	1.20E+02
Cu	*< 2.91E+01*	--	*< 9.65E+00*
Fe	*< 2.07E+01*	--	*< 7.72E+00*
Gd	*< 2.53E+01*	--	7.84E+00
K	*< 8.93E+03*	--	1.67E+03
La	*< 1.88E+01*	--	*< 8.69E+00*
Li	*< 7.98E+01*	--	2.10E+01
Mg	*< 5.81E+01*	--	*< 1.93E+00*
Mn	*< 2.07E+01*	--	*< 2.89E+00*
Mo	*< 1.91E+02*	--	1.06E+02
Na	2.18E+05	4E+03	2.16E+05
Ni	*< 7.03E+01*	--	*< 4.34E+01*
P	7.50E+02	9.8E+01	6.47E+02
Pb	*< 2.31E+02*	--	*< 2.76E+02*
S	2.49E+03	7E+01	1.98E+03
Sb	*< 1.42E+02*	--	7.54E+01
Si	*< 3.47E+01*	--	*< 2.42E+01*
Sn	*< 2.30E+02*	--	*< 1.10E+02*
Sr	*< 9.38E+01*	--	*< 7.72E+00*
Ti	*< 5.63E+00*	--	*< 1.25E+01*
V	*< 1.03E+01*	--	1.22E+01
Zn	1.05E+03	2E+01	7.61E+02
Zr	*< 1.13E+01*	--	*< 1.35E+01*

Table 20: Drained Interstitial Liquid ICP-MS results (mg/L)

Tank 10H	HTF-609 IL		HTF-610 IL
(mg/L)	Average	St. Dev.	
Mass 59	3.1E-01	2E-02	5.0E-01
Mass 88	*< 1.4E-01*	--	4.61E-02
Mass 99	8.80E+00	6E-02	1.26E+01
Mass 101	1.81E+00	3E-02	2.73E+00
Mass 133	2.09E+01	4E-01	2.92E+01
Mass 135	2.74E+00	9E-02	3.67E+00
Mass 137	1.02E+01	2E-01	1.29E+01
Mass 138	*< 2.0E-02*	--	*< 9.2E-02*
Mass 230	*< 1.3E-01*	--	*< 6.7E-02*
Mass 231	*< 1.3E-01*	--	*< 6.7E-02*
Mass 232	*< 1.3E-01*	--	*< 6.7E-02*
Mass 233	*< 1.3E-01*	--	*< 6.7E-02*
Mass 234	*< 1.3E-01*	--	*< 6.7E-02*
Mass 235	1.8E-01	3E-02	2.0E-01
Mass 236	*< 1.3E-01*	--	7E-02
Mass 237	*< 1.3E-01*	--	*< 6.7E-02*
Mass 238	1.21E+00	7E-02	1.24E+00
Mass 239	*< 1.3E-01*	--	*< 6.7E-02*
Mass 240	*< 1.3E-01*	--	*< 6.7E-02*
Mass 241	*< 1.3E-01*	--	*< 6.7E-02*
Mass 242	*< 1.3E-01*	--	*< 6.7E-02*
Mass 243	*< 1.3E-01*	--	*< 6.7E-02*
Mass 244	*< 1.3E-01*	--	*< 6.7E-02*
Total U	1.39E+00	1E-01	1.51E+00
^{235}U enrich	13.1%	0.9%	14.0%

Table 21: Tank 10H drained saltcake dissolution information and analysis of dissolved saltcake for radiochemical and ionic components.

Sample HTF-609	1st	2nd	3rd	4th	5th	6th	Bulk	
Time (min)	7 to 9	17 to 19	27 to 29	44 to 46	61 to 63	81 to 83	2 to 83	
Flow Rate (mL/min)	2.8	2.9	2.9	2.8	2.7	2.7	--	
Volume (mL)	20 to 25	45 to 50	70 to 75	115 to 120	160 to 165	225 to 230	0 to 230	
Density (g/mL)	1.32	1.28	1.28	1.26	1.21	1.16	1.23	
Radioisotopic Composition (pCi/mL)							avg.	st.dev.
^{90}Sr	--	--	--	--	--	--	8.08E+04	2.8E+03
^{99}Tc minimum	6.28E+03	5.01E+03	2.74E+03	2.54E+03	2.63E+03	9.14E+02	4.94E+03	3.6E+02
^{99}Tc maximum	8.39E+03	6.60E+03	4.62E+03	4.33E+03	3.82E+03	3.11E+03	5.78E+03	2.4E+02
^{137}Cs	6.70E+07	3.30E+07	3.10E+07	2.35E+07	1.74E+07	1.48E+07	2.55E+07	5E+05
^{238}Pu	6.64E+04	8.10E+04	7.76E+04	7.76E+04	8.63E+04	9.94E+04	4.77E+03	6E+01
$^{239/240}Pu$	9.72E+02	5.23E+03	1.05E+03	1.09E+03	8.69E+01	1.02E+03	3.78E+02	2.81E+02
^{241}Am	7.59E+02	6.42E+02	6.61E+02	5.64E+02	8.03E+02	9.42E+02	2.07E+02	1.6E+01
Ionic Composition (M)							avg.	st.dev.
Na^+	6.35E+00	5.59E+00	5.38E+00	5.15E+00	3.99E+00	3.09E+00	4.27E+00	2E-02
NO_3^-	3.03E+00	2.71E+00	2.49E+00	3.00E+00	2.43E+00	2.12E+00	2.15E+00	2.6E-01
NO_2^-	1.29E-01	6.24E-02	5.60E-02	6.75E-02	6.65E-02	2.74E-02	5.72E-02	8.4E-04
OH^-	2.16E-01	6.98E-01	8.19E-01	6.24E-01	2.33E-01	*< 9.90E-02*	8.20E-02	1.34E-02
AlO_2^-	4.74E-02	2.67E-02	2.48E-02	1.94E-02	1.37E-02	1.14E-02	1.95E-02	4E-04
CO_3^{2-}	2.29E-01	4.72E-01	2.07E-01	2.36E-01	3.62E-01	3.30E-02	3.94E-01	3.93E-03
SO_4^{2-}	5.79E-01	7.29E-01	6.86E-01	9.31E-01	5.59E-01	4.94E-01	5.03E-01	5.0E-02
PO_4^{3-}	*< 8.03E-03*	*< 7.38E-03*	*< 7.54E-03*	*< 7.78E-03*	*< 7.16E-03*	*< 6.02E-03*	*</=2.16E-03*	1.02E-03
Cl^-	*< 4.30E-03*	*< 3.95E-03*	*< 4.04E-03*	*< 4.17E-03*	*< 3.84E-03*	*< 3.23E-03*	*< 1.55E-03*	--
F^-	*< 8.03E-03*	*< 7.37E-03*	*< 7.54E-03*	*< 7.78E-03*	*< 7.16E-03*	*< 6.02E-03*	*< 2.88E-03*	--
$C_2O_4^{2-}$	*< 8.66E-03*	*< 7.96E-03*	*< 8.13E-03*	*< 8.40E-03*	*< 7.72E-03*	*< 6.50E-03*	*</=2.33E-03*	1.10E-03
CHO_2^-	*< 1.69E-02*	*< 1.56E-02*	*< 1.59E-02*	*< 1.64E-02*	*< 1.51E-02*	*< 1.27E-02*	*< 6.09E-03*	--
Total Base	3.88E-01	1.05E+00	1.17E+00	1.00E+00	6.50E-01	*< 9.90E-02*	5.41E-01	2.2E-02
K^+	*< 1.85E-02*	1.64E-02	1.76E-02	*< 1.59E-02*	*< 1.58E-02*	*< 1.29E-02*	*</=7.42E-03*	2.52E-03

Table 22: Analysis of drained and dissolved Tank 10H saltcake for elemental components

Sample HTF-609	1st	2nd	3rd	4th	5th	6th	Bulk	
Other Elemental Composition (mg/L)							avg.	st.dev.
Ag	*< 3.26E+00*	*< 2.79E+00*	*< 2.78E+00*	*< 2.80E+00*	*< 2.78E+00*	*< 2.28E+00*	*< 9.93E-01*	--
As	--	--	--	--	--	--	--	--
B	*< 5.39E+01*	*< 4.60E+01*	*< 4.58E+01*	*< 4.62E+01*	*< 4.59E+01*	*< 3.76E+01*	*< 1.64E+01*	--
Ba	*< 4.08E+00*	*< 3.48E+00*	*< 3.47E+00*	*< 3.51E+00*	*< 3.47E+00*	*< 2.84E+00*	1.56E+00	1.3E-01
Ca	1.47E+01	1.52E+01	9.92E+00	1.21E+01	1.03E+01	7.94E+00	7.94E+00	1.92E+00
Cd	*< 9.80E+00*	*< 8.35E+00*	*< 8.34E+00*	*< 8.41E+00*	*< 8.33E+00*	*< 6.83E+00*	*< 2.98E+00*	--
Ce	4.76E+01	3.54E+01	4.21E+01	3.74E+01	3.54E+01	*< 2.90E+01*	2.36E+01	4.18E+00
Co	1.85E-01	*< 1.17E-01*	*< 1.18E-01*	*< 1.23E-01*	*< 1.30E-01*	*< 1.94E-01*	1.06E-01	3E-03
Cr	*< 3.26E+01*	*< 2.79E+01*	*< 2.78E+01*	*< 2.80E+01*	*< 2.78E+01*	*< 2.28E+01*	*< 9.93E+00*	--
Cs	1.89E+00	9.48E-01	9.21E-01	6.93E-01	5.46E-01	4.73E-01	1.02E+00	4E-02
Cu	*< 8.17E+00*	*< 6.96E+00*	*< 6.94E+00*	*< 7.01E+00*	*< 6.95E+00*	*< 5.70E+00*	*< 2.49E+00*	--
Fe	*< 6.54E+00*	*< 5.56E+00*	*< 5.55E+00*	*< 5.60E+00*	*< 5.56E+00*	*< 4.55E+00*	*< 1.98E+00*	--
Gd	*< 6.54E+00*	*< 5.56E+00*	*< 5.55E+00*	*< 5.60E+00*	*< 5.56E+00*	*< 4.55E+00*	2.89E+00	6.4E-01
Hg	--	--	--	--	--	--	--	--
La	9.00E+00	*< 6.27E+00*	*< 6.24E+00*	*< 6.31E+00*	*< 6.25E+00*	*< 5.12E+00*	3.23E+00	3.6E-01
Li	1.61E+01	1.19E+01	1.47E+01	1.21E+01	1.01E+01	7.21E+00	8.08E+00	1.03E+00
Mg	*< 1.63E+00*	*< 1.39E+00*	*< 1.39E+00*	*< 1.41E+00*	*< 1.39E+00*	*< 1.14E+00*	*< 4.96E-01*	--
Mn	*< 2.45E+00*	*< 2.09E+00*	*< 2.08E+00*	*< 2.10E+00*	*< 2.09E+00*	*< 1.71E+00*	*< 7.45E-01*	--
Mo	*< 5.47E+01*	*< 4.66E+01*	*< 4.65E+01*	*< 4.70E+01*	*< 4.66E+01*	*< 3.81E+01*	*< 1.66E+01*	--
Ni	*< 3.67E+01*	*< 3.13E+01*	*< 3.13E+01*	*< 3.15E+01*	*< 3.13E+01*	*< 2.57E+01*	*< 1.12E+01*	--
P	*< 3.42E+02*	*< 2.91E+02*	*< 2.91E+02*	*< 2.94E+02*	*< 2.91E+02*	*< 2.38E+02*	*< 1.04E+02*	--
Pb	*< 2.34E+02*	*< 1.99E+02*	*< 1.99E+02*	*< 2.01E+02*	*< 1.99E+02*	*< 1.63E+02*	*< 7.09E+01*	--
S	2.08E+04	2.25E+04	2.27E+04	2.30E+04	1.54E+04	1.19E+04	1.77E+04	9E+01
Sb	*< 5.80E+01*	*< 4.94E+01*	*< 4.93E+01*	*< 4.98E+01*	*< 4.94E+01*	*< 4.05E+01*	*< 1.76E+01*	--
Se	--	--	--	--	--	--	--	--
Si	*< 2.04E+01*	*< 1.73E+01*	*< 1.74E+01*	*< 1.75E+01*	*< 1.73E+01*	*< 1.42E+01*	*< 6.21E+00*	--
Sn	*< 9.32E+01*	*< 7.94E+01*	*< 7.91E+01*	*< 7.99E+01*	*< 7.92E+01*	*< 6.50E+01*	*< 2.83E+01*	--
Sr	*< 6.54E+00*	*< 5.56E+00*	*< 5.55E+00*	*< 5.60E+00*	*< 5.56E+00*	*< 4.55E+00*	*< 1.98E+00*	--
Ti	*< 1.06E+01*	*< 9.04E+00*	*< 9.02E+00*	*< 9.11E+00*	*< 9.04E+00*	*< 7.40E+00*	*< 3.23E+00*	--
V	*< 8.99E+00*	*< 7.65E+00*	*< 7.63E+00*	*< 7.70E+00*	*< 7.64E+00*	*< 6.26E+00*	*< 2.73E+00*	--
Zn	9.91E+01	5.10E+01	4.46E+01	2.98E+01	1.87E+01	2.46E+01	4.46E+01	6E-01
Zr	*< 1.14E+01*	*< 9.73E+00*	*< 9.71E+00*	*< 9.81E+00*	*< 9.73E+00*	*< 7.98E+00*	*< 3.47E+00*	--

Table 23: Analysis of drained and dissolved Tank 10H saltcake by ICP-MS.

Sample HTF-609	1st	2nd	3rd	4th	5th	6th	Bulk	
ICP-MS (mg/L)							avg.	st.dev.
Mass 59 (Co)	1.85E-01	*< 1.17E-01*	*< 1.18E-01*	*< 1.23E-01*	*< 1.30E-01*	*< 1.94E-01*	1.06E-01	3E-03
Mass 88 (Sr)	3.70E-02	3.53E-01	3.84E-02	4.05E-02	3.29E-02	2.52E-02	5.71E-02	8E-05
Mass 99 (Tc,Ru)	4.95E-01	3.90E-01	2.73E-01	2.55E-01	2.26E-01	1.84E-01	3.41E-01	1.4E-02
Mass 101 (Ru)	1.66E-01	1.26E-01	1.49E-01	1.41E-01	9.44E-02	1.73E-01	6.62E-02	9.6E-03
Mass 133 (Cs)	1.12E+00	5.68E-01	5.65E-01	4.23E-01	3.46E-01	3.03E-01	7.30E-01	2.9E-02
Mass 135 (Cs,Ba)	1.43E-01	7.98E-02	6.22E-02	5.46E-02	4.80E-02	4.25E-02	9.48E-02	4.3E-03
Mass 137 (Cs,Ba)	5.60E-01	3.67E-01	3.46E-01	3.00E-01	2.43E-01	2.29E-01	4.15E-01	2.1E-02
Mass 138 (Ba)	*< 4.53E-02*	*< 4.05E-02*	*< 4.09E-02*	*< 4.26E-02*	*< 4.53E-02*	*< 6.75E-02*	*< 2.38E-02*	--
Mass 230 – 231	*< 3.30E-02*	*< 2.95E-02*	*< 2.98E-02*	*< 3.10E-02*	*< 3.30E-02*	*< 4.92E-02*	*< 1.73E-02*	--
Mass 232 (Th,U)	4.74E-02	6.24E-02	4.59E-02	5.85E-02	7.95E-02	8.71E-02	*< 1.73E-02*	--
Mass 233 (U)	8.85E-02	1.15E-01	9.76E-02	7.13E-02	8.05E-02	7.68E-02	*< 1.73E-02*	--
Mass 234 (U)	*< 3.30E-02*	*< 2.95E-02*	*< 2.98E-02*	*< 3.10E-02*	*< 3.30E-02*	*< 4.92E-02*	*< 1.73E-02*	--
Mass 235 (U)	5.51E-01	4.29E-01	4.50E-01	3.74E-01	3.29E-01	3.70E-01	3.09E-02	4.1E-03
Mass 236 (U)	1.36E-01	1.14E-01	1.12E-01	8.69E-02	7.79E-02	8.67E-02	*< 1.73E-02*	--
Mass 237 (Np)	9.02E-02	7.48E-02	8.66E-02	6.69E-02	4.94E-02	6.99E-02	*< 1.73E-02*	--
Mass 238 (U,Pu)	4.18E+00	3.62E+00	3.77E+00	2.89E+00	2.39E+00	2.97E+00	2.72E-01	7.0E-02
Mass 239 (Pu)	5.04E-02	5.21E-02	4.80E-02	4.45E-02	3.69E-02	4.69E-02	*< 1.73E-02*	--
Mass 240 – 245	*< 3.30E-02*	*< 2.95E-02*	*< 2.98E-02*	*< 3.10E-02*	*< 3.30E-02*	*< 4.92E-02*	*< 1.73E-02*	--
Unanium Summary							avg.	st.dev.
Total U (mg/L)	4.95E+00	4.28E+00	4.43E+00	3.42E+00	2.88E+00	3.50E+00	3.03E-01	7.4E-02
^{235}U enrichment (%)	11.1%	10.0%	10.2%	11.0%	11.4%	10.6%	10.3%	1.2%

Table 24: Likely major components of Tank 10H salt solids, normalized to 100%.

(wt %)	HTF-610	HTF-611
$NaNO_3$	34.7	93.8
Na_2CO_3	41.0	2.4
Na_2SO_4	24.3	3.8

Table 25: Washing of the top portion of sample HTF-609

Analyte	Units	Sample 1	Sample 2	Sample 3	Sample 4	Sample 5	Sample 6
^{99}Tc	pCi/mL	4.33E+04	3.68E+04	3.32E+04	2.28E+04	1.08E+04	4.12E+03
^{137}Cs	pCi/mL	2.16E+08	1.85E+08	1.65E+08	1.12E+08	5.42E+07	1.86E+07
^{238}Pu	pCi/mL	1.23E+04	8.51E+03	8.20E+03	1.32E+04	6.43E+03	2.05E+04
^{235}U	mg/L	1.06E-01	9.14E-02	9.60E-02	5.23E-02	3.71E-02	1.25E-01
^{238}U	mg/L	1.05E+00	8.27E-01	6.78E-01	5.91E-01	4.01E-01	2.48E+00
Na^+	M	10.0	10.3	10.3	10.5	10.4	10.5
AlO_2^-	M	0.148	0.126	0.109	0.078	0.0377	0.0146
SO_4^{2-}	M	0.0381	0.0348	0.0352	0.0339	0.0335	0.0259
PO_4^{3-}	M	0.0113	< 0.0105	< 0.0108	< 0.0110	< 0.0107	< 0.0106
Ba	mg/L	5.26E+00	3.99E+00	*< 3.99E+00*	4.26E+00	4.31E+00	4.73E+00
Ca	mg/L	1.29E+01	*< 9.34E+00*	*< 9.56E+00*	*< 9.73E+00*	*< 9.46E+00*	1.03E+01
Ce	mg/L	7.55E+01	4.93E+01	5.25E+01	4.61E+01	5.98E+01	7.27E+01
Cr	mg/L	3.54E+01	3.35E+01	*< 3.19E+01*	*< 3.25E+01*	*< 3.15E+01*	*< 3.12E+01*
Cu	mg/L	4.05E+01	3.53E+01	3.15E+01	1.90E+01	*< 7.88E+00*	*< 7.83E+00*
Fe	mg/L	2.66E+01	1.92E+01	2.03E+01	1.75E+01	2.51E+01	1.62E+01
K	mg/L	*< 7.34E+02*	1.08E+03	*< 7.07E+02*	*< 7.20E+02*	*< 7.00E+02*	1.33E+03
Li	mg/L	2.58E+01	1.69E+01	1.54E+01	1.48E+01	1.78E+01	2.34E+01
Mn	mg/L	4.40E+00	3.26E+00	2.53E+00	*< 2.44E+00*	2.60E+00	8.89E+00
Si	mg/L	5.26E+01	5.01E+01	6.37E+01	4.98E+01	5.54E+01	5.21E+01
Zn	mg/L	4.65E+02	3.92E+02	3.39E+02	2.30E+02	1.02E+02	2.55E+01